International
Progress Report

IPR-04-11

# Äspö Hard Rock Laboratory

## Prototype Repository

## Comparison of results from THMCB modelling of buffer, backfill and rock with measured data from Prototype Repository

## D35

Roland Pusch

Geodevelopment AB

February 2004

**Svensk Kärnbränslehantering AB**
Swedish Nuclear Fuel
and Waste Management Co
Box 5864
SE-102 40 Stockholm Sweden
Tel 08-459 84 00
+46 8 459 84 00
Fax 08-661 57 19
+46 8 661 57 19


Äspö Hard Rock
Laboratory

Report no.
IPR-04-11
No.
F63K
Author
Roland Pusch
Date
Feb.2004
Checked by
Date

Approved
Christer Svemar
Date
2005-04-25

# Äspö Hard Rock Laboratory

## Prototype Repository

## Comparison of results from THMCB modelling of buffer, backfill and rock with measured data from Prototype Repository

## D35

Roland Pusch

Geodevelopment AB

February 2004

*Keywords:* Prototype Repository, THMCB, Modelling Buffer, Backfill, Rock


# PROTOTYPE REPOSITORY

*Deliverable D 35*

## Comparison of results from THMCB m odelling of buffer, backfill and rock with measured data from Prototype Repository

**D35**

Editor

Roland Pusch

Geodevelopment AB

February 2004

EC Contract FIKW-2000-00055

EC-5th EURATOM Framework programme 1998-2002
Key Action: Nuclear Fission

# Summary

The purpose of the work has been to compare predictions made by applying the theoretical models with actual measurements and the following major conclusions can be drawn:

- The geohydraulic and geochemical modellings refer to stages that have not yet been reached in the repository test area and no safe conclusions concerning their applicability can yet be made. Predictions of access to water from the rock in the deposition holes are uncertain and future work related to rock structure on different scales appears to be required for adequate modelling of the hydration of buffers and backfills.

- All the theoretical models give data that are on the same order of magnitude as the measurements and can be used for rough prediction of the temperature, hydration and pressure build-up in buffer of the type used in the Prototype Repository Project.

- Best agreement between predictions and measurements is obtained for the temperature evolution. Some models overestimate the temperature for the first two years, hence yielding a safe, conservative prediction, while the others give very accurate forecasting. There are indications that the thermal conductivity of the buffer is higher than assumed and that the heat transfer is assisted by some undefined mechanism like convection through vapour flow.

- The hydration rate is more difficult to predict than temperature. A first and major problem is the risk of water migration along cables to moisture sensors, which may have given incorrect information on the rate of hydration of un-instrumented buffer. Thus, the reference values to be compared with the predictions may not be adequate. Disregarding from this it is concluded that almost all the models have yielded data that are fairly well in agreement with the recordings and that the models provide sufficiently safe information on the wetting rate for practical use concerning deposition holes with “unlimited” access to water from the rock. The predicted rate of saturation is generally too high, indicating that all processes involved in the moistening are not fully understood.

- For deposition holes with limited access to water for hydration the situation is more uncertain. One of the models could fairly accurately predict the hydration in a “dry” hole by basing the calculation on measured inflow before applying the buffer in the hole (No 3), but it seems more difficult to foresee the wetting in planning a repository with much less information on the hydraulic performance of the near-field rock. This matter should be in focus in future R&D.

- The evolution of pressure and mechanical response of the buffer is the most difficult task because it requires that fracturing and displacements in the buffer be included in the models and that the interrelation of hydration/dehydration and swelling/drying are relevant. Since prediction of the hydration rate appears to be uncertain forecasting of the mechanical response is even more uncertain. However, the models manage to give data that are not too different from the recordings and that are sufficiently accurate for practical purposes. Like for the hydration some pressure gauges may have reacted too soon because of water migration along cables and this may imply that the maturation of the buffer is in fact even slower than indicated by the recordings. The evolution of pressure in the buffer in "dry" deposition holes is even more difficult to predict but stable conditions may require several tens of years according to models like the one proposed by BGR.

# Sammanfattning

Ändamålet med arbetet har varit att jämföra förutsägelser av närfältprocesser framtagna med hjälp av teoretiska modeller med verkliga värden och det har lett till följande slutsatser:

- Geohydrologiska och geokemiska modelleringar hänför sig till stadier som ännu inte nåtts i testområdet och inga säkra slutsatser rörande deras giltighet kan ännu dras. Prediktion av vattentillgången i deponeringshålen är osäker och man finner att mer arbete med frågan, kopplat till bergets struktur, är nödvändigt i framtiden för att kunna göra adekvat modellering av bevätningen hos buffert och återfyllning.

- Alla teoretiska modeller ger data av samma storleksordning som mätresultaten och kan användas för ungefärlig förutsägelse av temperatur, bevätning och tryckuppbyggnad i buffert av den typ som används i Prototypförsöket.

- Den bästa överensstämmelsen mellan prediktion och verklighet fås för temperaturutvecklingen. Vissa modeller överskattar dock temperaturen för de två första åren, innebärande konservativa resultat, medan de andra ger mycket god överensstämmelse med mätdata. Det kan finnas skäl att anta att värmeledningsförmågan hos bufferten är högre än som antagits och att det möjligen kan bero på bättre värmetranstort genom t ex ångkonvektion.

- Bevätningshastigheten är svårare att förutsäga än temperaturen. Ett första och avgörande problem är risken för vattenvandring utmed kablar till fuktmätarna, vilket kan ge felaktig information om hur bevätningshastigheten är hos buffert som inte har instrumentering. Sålunda kan de experimentella referensvärdena vara felaktiga. Om man bortser härifrån är bedömningen att nästan alla modeller gett data som stämmer relativt väl med förutsägelserna och att de kan ge tillräckligt säkert besked om förväntad bevätningstakt hos bufferten i deponeringshål med ”obegränsad” tillgång till vatten. Dock är hastigheten i princip överskattad vilket innebär att processerna som styr bevätningen inte är helt klarlagda.

- För deponeringshål med begränsad eller ringa tillgång till vatten från berget är situation mera osäker. En av modellerna kunde ge en någorlunda väl överensstämmande förutsägelse av bevätningstakten i ett ”torrt” hål grundat på inflödet i hålet före anbringandet av bufferten (Hål No 3), men det bedöms vara svårare att göra sådana prognoser vid planeringen av ett framtida slutförvar med mycket mindre information om närfältbergets hydrauliska egenskaper. Denna fråga bör vara i fokus i fortsatt FoU-arbete.

- Utvecklingen av tryck och mekanisk funktion hos bufferten är den svåraste modelleringsuppgiften därför att man måste införa sprickbildning och inre förskjutningar i modellerna och se till att kopplingen mellan bevätning/uttorkning och svällning/krympning blir relevant. Eftersom förutsägelse av bevätningstakten är osäker är bedömningen av tryckuppbyggnad och mekanisk funktion ännu svårare. Dock kunde modellerna ge prediktioner som inte avvek starkt från mätvärdena och som kan vara tillräckligt säkra för praktiska ändamål. Liksom fuktmätarna kan tryckgivarna ha gett för snabb reaktion och det kan innebära att mognaden hos icke instrumenterad buffert i själva verket är ännu långsammare än vad mätningarna visar. Tryckutvecklingen i ”torra” deponeringshål är ännu svårare att förutse och stabilt tillstånd kan ta åtskilliga tiotals år enligt vissa modeller, t ex den som föreslagits av BGR.

# Contents

# 1 Background

The main objectives of the Prototype Repository Project are to simulate part of a future KBS-3 Deep Repository, to develop and test appropriate engineering standards, and to demonstrate the integrated function of repository components and to compare results with predictive calculations based on conceptual and theoretical models.

An important objective is to accomplish confidence building as to the capability of modelling EBS performance by providing data, which are used by the participants for demonstrating their ability to predict the performance of barriers with models that are developed for somewhat different conditions than those in the AEspoe URL. Document D35 is focused on the issue of comparing results from predicting the performance of buffer and backfill in the Prototype Repository Project using THMCB models and actually obtained field data.

# 2 Structure of report

## 2.1 Activities in Work Packages

The work in the respective work packages have comprised the following activities:

**WP1**

WP1a: Measurement of THM processes in buffer and backfill

WP1b: Measurement of hydraulic regimes in the rock

WP1c: Measurement of the mechanical conditions in the rock

WP1d: Geochemistry, gas and biology of buffer and backfill

WP1e: Resistivity measurements

WP1f: Displacements of canisters

*The report primarily deals with field data and modelling in WP1a, WP1b, WP1d and WP1f.*

**WP2**

WP2a: Preparation of deposition holes and installation of sensors

WP2b: Emplacement of buffer and disposal of canisters

WP2c: Emplacement of backfills

*Since no modelling has been made in this work package it is not dealt with in the report.*

**WP3**

WP3a: Water and gas sampling and analysis

WP3b: Hydraulic tests in rock

WP3c: THM laboratory tests on buffer and backfill properties

WP3d: Laboratory tests on mechanical properties of rock and THM processes in rock

WP3e: Laboratory determination of cracks in EDZ

WP3f: T and TM modelling

WP3g: HM and THM modelling of rock mass

WP3h: THM modelling of buffer and backfill, and interaction with near-field rock

WP3i: C modelling of buffer, backfill and groundwater

*The report primarily deals with field data and modelling in WP3b, WP3h and WP3i.*

## 2.2 Presentation of data and modellings

The main purpose of the present document, i.e. to compare predicted and actually obtained field data and evaluate discrepancies, is made for each separate sub-package for the sake of clarity. Hence, for the buffer and backfill measurements obtained in WP1a are compared with the results of modellings in WP3h etc, according to Table 2-1.

**Table 2-1. Basis of comparison of predicted and actual field data.**

| **Subject** | **Data from WP1 compared with Data from WP3** | |
|---|---|---|
| | **WP1 (Actual data)** | **WP3 (Modelling)** |
| *Rock performance* | * Hydraulic regimes in rock (WP1b) | * HM and THM modelling of rock (WP3g) |
| *Buffer and backfill* | * THM Processes in buffer and backfill (WP1a)<br>* Canister displacement (WP1f)<br>* Buffer chemistry (TC), WP1d | * THM modelling of buffer and backfill, and interaction with near-field rock (WP3h)<br>* C modelling of buffer, backfill and groundwater (WP3i) |

# 3 Rock conditions

## 3.1 Far-field conditions

### *Large-scale rock structure*

Preceding work on characterization of the general rock structure in terms of location, orientation and properties of fracture zones and rock matrix [3-1], led to definition of 18 deterministic discontinuities ("structures") and the way they perform hydraulically [3-2]. Groundwater flow is concentrated to discrete, interacting fracture zones of different size and extension in the far-field and to systems of discrete fractures in the near-field.

The most important conclusion from the studies is that tracer movement is – as expected – closely related to the existence of major hydraulically active features identified and characterized discontinuities.

### *Piezometric predictions*

One of the most important factors that determine the hydration rate of buffers and backfills is the groundwater pressure, which has been calculated by Rhen et al (Figure 3-1). The rock between major water-bearing features on all scales has a low hydraulic conductivity and the concept of "porous medium" water flow is believed to be applicable. As an average, the hydraulic conductivity in the interval 300-500 m depth is concluded to range between E-11 and E-9 m/s, while the average conductivity of major fracture zones varies between E-9 and E-6 m/s.

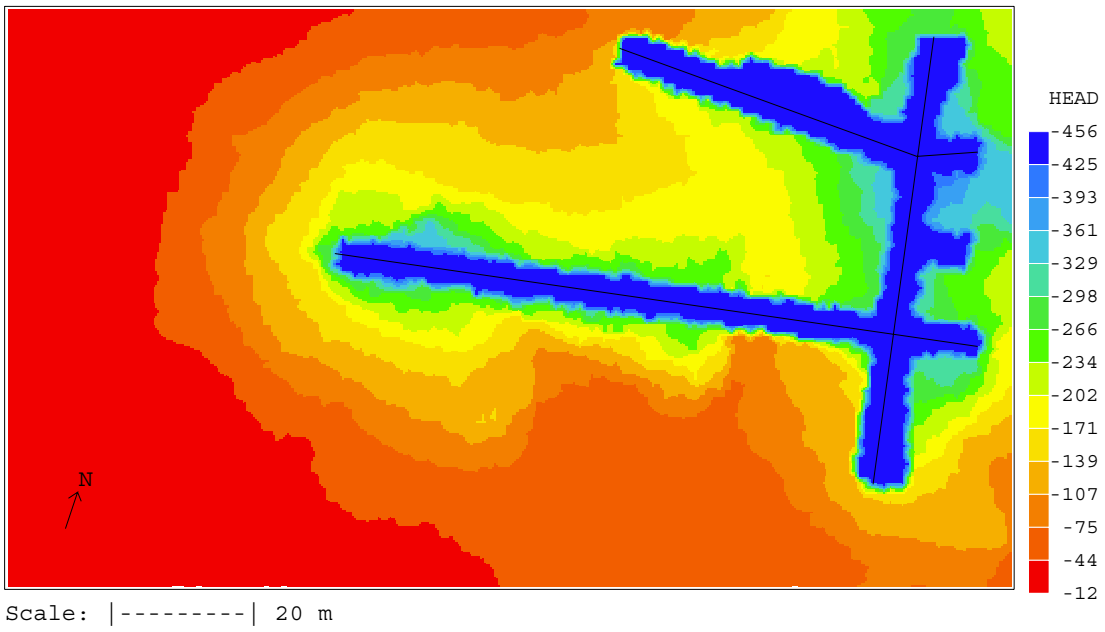


***Figure 3-1.*** *Predicted pressure heads in meters at 447 m depth in granite at AEspoe URL [3-2].*

### *Comparison of predicted and recorded far-field pressure data*

It is concluded that the applied way of predicting groundwater pressures on a large scale taking fracture zones as discrete hydraulically active discontinuities into consideration gives values that are in fair agreement with recordings.

## 3.2 Near-field conditions – pressure

### *Prediction of pressures*

Modelling of groundwater pressure in the near-field using the same code as for the large-scale hydrological modelling has given a water pressure at 2 m distance from the tunnel wall between 100 kPa and 1.5 MPa.

### *Recorded pressures*

The actual pressures measured in the rock surrounding the Prototype Repository drift are within the same large span as the predictions.

## 3.3 Near-field conditions – hydraulic conductivity

### *Prediction and evaluation of the bulk hydraulic conductivity of the near-field rock*

A recent attempt by Golders to predict the inflow of water into the deposition holes of the Prototype Repository Project using the code DFN has given the data in Table 3-2, which also gives recorded inflows [3-3]. The fracture system used in the model was based on trace maps defined from visual inspections of the 1.75 m diameter holes with 8 m depth. The discrepancy between predictions and recordings is substantial.

**Table 3-2. Comparison of measured and calculated inflow to deposition holes.**

| Hole No | Designation | Predicted median inflow, l/min | Recorded inflow, l/min |
|---|---|---|---|
| 1 | DA3587G01 | 0.943 | 0.0800 |
| 2 | DA3581G01 | 0.553 | 0.0020 |
| 3 | DA3575G01 | 0.607 | 0.0030 |
| 4 | DA3569G01 | 0.695 | 0.0007 |
| 5 | DA3551G01 | 1.678 | 0.0027 |
| 6 | DA3545G01 | 0.934 | 0.0030 |

The inflow of water into the large-diameter deposition holes would correspond to the hydraulic conductivities of the near-field rock shown in Table 3-3 according to Rhen et al. A geometric mean of these values is slightly higher than E-11 m/s excepting the hole with the discrete fracture, and somewhat higher than E-10 m/s including it.

**Table 3-3. Inflow in large deposition holes or boreholes and corresponding theoretical hydraulic conductivity of the near-field rock. Flows into borehole (ca 0.1 to 0.0001 liter/min) at positions of deposition holes and into deposition holes (ca 0.1 to 0.001 l/min) in the range as measured [3-2]. (Assumptions: Radial flow. Borehole diameter 76 mm, Deposition hole diameter 1.75 m, Pressure difference of 2000 kPa from the hole to a point at a distance of 10 m. Borehole/deposition hole length 8 m).**

| Deposition hole inflow (l/min) | Borehole inflow (liter/min) | Mean hydraulic conductivity of rock (m/s) |
|---|---|---|
| 0.00035 | 0.00011 | E-12 |
| 0.0035 | 0.0011 | E-11 |
| 0.035 | 0.011 | E-10 |
| 0.35 | 0.11 | E-9 |
| 0.044 | 0.014 | E-12 and a fracture with transmissivity E-9 $m^2/s$ |
| 0.43 | 0.14 | E-12 and a fracture with transmissivity E-8 $m^2/s$ |

The conductivity of the rock closest to the drift and deposition holes determines how the water inflow into these openings is distributed. Excavation-disturbed zones caused by TBM boring perform as porous media and various investigations performed by GBR, Posiva, and SKB indicate that the average hydraulic conductivity within about 10 mm from borehole walls is about E-10 to E-9 m/s, and that it is E-11 to E-10 m/s for the rock within a couple of decimetres from the wall. This agrees well with the bulk hydraulic data just mentioned.

### *Comparison of predicted and recorded near-field conductivity data*

Comparison of predicted and calculated inflow in the six deposition holes showed very poor agreement as illustrated by the data in Table 3-2. The reason for the misfit may be that just one or a couple of water-bearing fractures control the inflow and that significant flow paths are those represented by crossing fractures of this type. Examples of similar type from the very tight granite at AECL's URL in Canada provided by OPG, using the codes COMPASS and FLAC for rock characterization, shows somewhat better but still rather poor agreement.

It is believed that further development of the structure models should be made for safer prediction of water flow to deposition holes and tunnels. Some help is provided by the finding from the URLs at Stripa and AEspoe that the most water-bearing discrete, major fractures are those oriented in the direction of the major primary horizontal stress in the rock, which is commonly the major principal stress.

## 3.4 Near-field conditions – electrolyte content in the groundwater

### *Prediction of the chemical constitution of the groundwater in the near-field rock and of the porewater of backfill and buffer*

On a broad scale the modelling task is divided into two parts (repository near-field and engineered barrier system). Analysed water samples from the near-field rock from March 1998 to June 1999 around the Sections 1 and 2 indicate small variations in the groundwater composition during the monitoring time. Inverse modelling calculations (made by use of PHREEQC-2.5 software) prove that the present groundwater surrounding the Prototype drift is almost completely of Baltic Sea origin. However, during infiltration through the sea bottom sediments and transport via the fracture zone network this water has altered significantly. Notable organic and cation exchange processes assigned to occur in the sea bottom sediments have modified the composition of the sea water. The hydraulic draw-down conditions remain fairly constant in the open AESpoe tunnel system and it is therefore predicted that no changes in the near-field groundwater composition that affect the Prototype Repository experiments will take place.

The predictive modelling calculations for the engineered barrier system (EBS) hence rely on the assumption of a constant near-field groundwater composition. The modelling within the EBS focuses on the major element concentrations in porewaters, and on certain solid phases (montmorillonite, quartz, calcite, gypsum, pyrite, goethite) in EBS components. The model computations follow equilibrium thermodynamic assumptions [3-4] and take into account also the known cation exchange properties of the EBS [3-5]. The calculations consider both reactions that occur during the wetting of the EBS interior, i.e. the buffer and backfill, and reactions that are related to time-dependent changes at the EBS boundaries. The available chemical information has been used for making the calculations as accurate as possible but significant simplifications had to been done as specified below.

1. The predictive computations assume that the initially unsaturated EBS pore spaces are filled with air. An instant complete saturation of the space is assumed to be caused as soon as infiltrating water starts entering it. All subsequent reaction cycles are assumed to occur in the saturated anoxic system.

2. The predictive calculations are batch reaction oriented, i.e. water entering EBS reaction space stays as long as required for complete chemical equilibration with respect to the minerals considered. No exact time frequencies were assumed for batch reaction cycles, i.e. the time-dependency of chemical changes are expressed only as functions of batch reaction cycles.

3. The presented prediction concept contains no exact estimates of how fast saturation (or partial saturation) takes place within the EBS (tunnel backfill or buffer). The gradual wetting of EBS is hence taken to be a separate hydrological TH problem.

Figure 3-2 shows an example of batch modelling yielding results representing the repository tunnel boundary. The geochemical evolution in material properties and resulting porewater compositions in the EBS at rock-backfill boundary are modelled as functions of batch reaction cycles. At the beginning of each cycle, a new unit volume of average near-field water enters in the backfill boundary cell. After geochemical equilibration, final porewater and solid phase compositions are defined.

The initially sub-saturated boundary space elements contain air (Figure 3-2). During the first fill-up of the cell, all oxygen from air is consumed by pyrite dissolution and simultaneous goethite precipitation. The two first reaction cycles dissolve all gypsum reserves, and at the same time a minute amount of calcite reserves is dissolved. During later cycles, however, minor calcite precipitation takes place in the cell because of the temperature gradient effect. Constant amounts of quartz are dissolved in porewater during each batch reaction cycle indicating that dissolved silica is carried away from the studied boundary space element. The resulting porewater compositions evolve as a function of batch reaction cycles because of mineral reactions, and because of significant cation exchange processes present in the system.

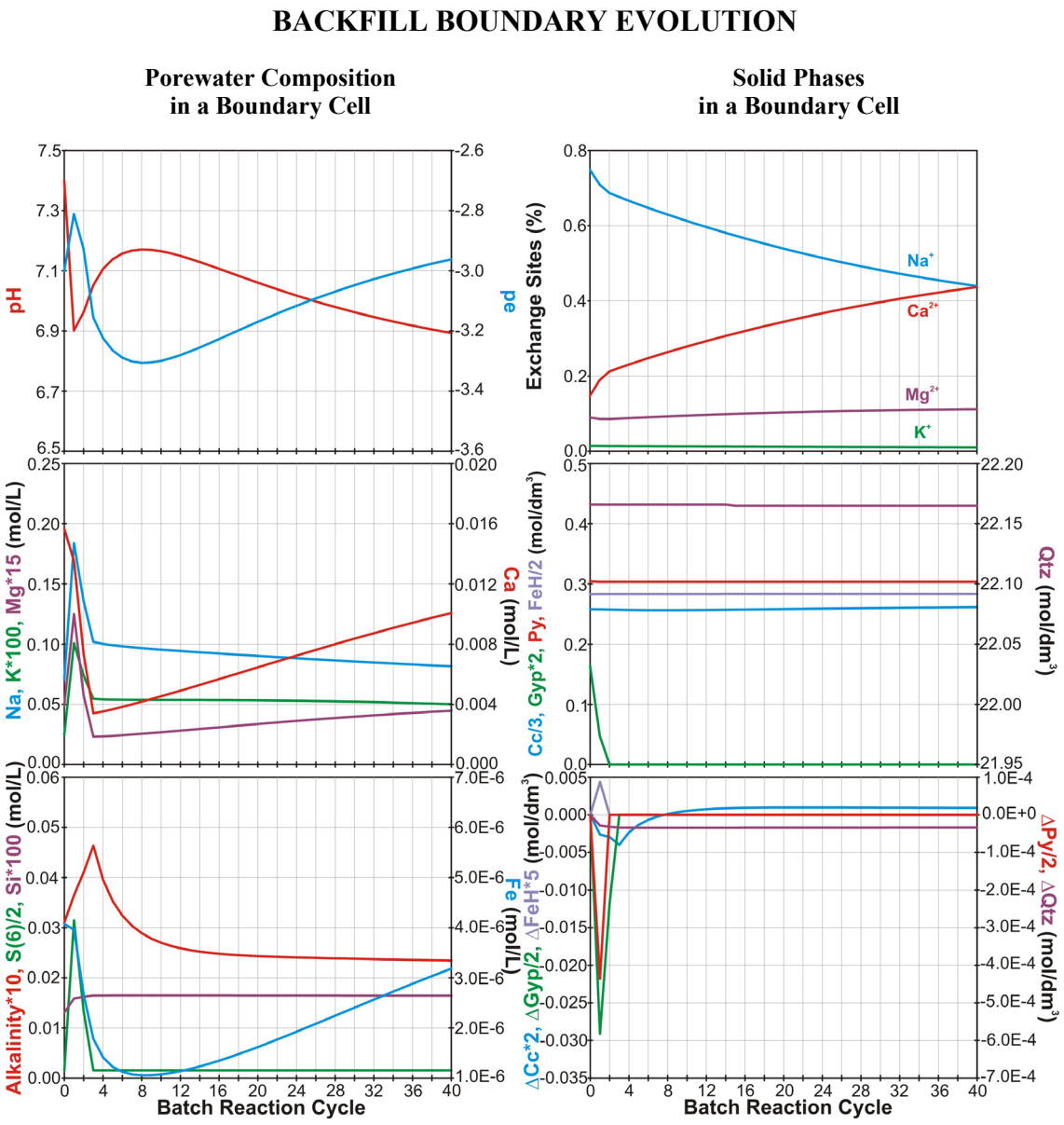


***Figure 3-2.*** *Geochemical evolution of material properties and resulting porewater compositions in an EBS element at the rock-backfill boundary. The volume is refilled 40 times with repository near-field water. The equilibrium temperature assumption is 40°C. Cc = calcite, Gyp = gypsum, Py = pyrite, FeH = goethite.*

As to the mineral dissolution/precipitation reactions the model predicts some calcite precipitation in the course of time at the boundaries of the repository tunnel. Similarly, quartz is dissolved from the repository boundary due to temperature gradient effect. However, as soon as temperature of porewater drops quartz will precipitate. Hence, a temperature-driven hydraulic convection shell may be generated around the repository that redistributes e.g. quartz.

### *Recording of the chemical constitution of the groundwater in the near-field rock and the porewater of backfill and buffer*

Due to delays in the repository operation (malfunctions in the canister heaters) the geochemical sampling program of the repository near-field and EBS has been delayed and for this reason the recordings of the chemical constitution of waters involved in the operating repository system are still missing. The porewater samplings from the EBS will be challenging tasks and no analytical results will be available before the end of EU-project.

### *Comparison of predictions of water geochemical data and other recordings*

It is estimated that the groundwater composition in the Prototype near-field will not undergo significant changes in the current experiment period. Future groundwater monitoring will show whether this is correct.

Considering the porewater of backfill and buffer the calculations are essentially "blind predictions". The modelling approach is simplified and not coupled to any large-scale quantitative flow model. However, porewater predictions are in conceptual agreement with several studies done elsewhere yielding information on the silica redistribution among other data [3-6]. The mineralogical observations of "long term test of buffer material (LOT)" –experiment [3-7] indicate that calcite precipitation as a result of temperature gradient is possible. Further, observations from the LOT-experiment and elsewhere [3-8] show that the sulphate levels in porewater are controlled and limited by the gypsum solubility limited, which is in agreement with the theoretical modelling. The modelling calculations are based on the assumption that the available oxygen in the unsaturated EBS is consumed in the pyrite dissolution process and not by microbial respiration. This deduction is in agreement with the results of Pedersen [3-9], who has stated that the amount of viable microbes decreases rapidly during swelling of the buffer bentonite thereby leading to eradication of life at water saturation.

The modelling results of the wetting of EBS interior are not considered in detail in this summary. However, it should be pointed out that the flow of water into unsaturated EBS raises the sulphate levels in the porewater and leads to gypsum precipitation. This has been confirmed by electron microprobe observations from samples extracted from the LOT-buffer columns [3-7].

# 4 Buffer and Backfill - THMC processes

## 4.1 Summary of theoretical models

The models used in predicting and evaluating the various processes in the Prototype Repository buffer and backfill have been described in detail in D33 and predictive modelling has been reported in the international Progress Report IPR-03-26. In the present document a brief summary of the major features of the models is given followed by examples of the most important processes:

1. Hydration of the buffer and backfill.
2. Build-up of swelling pressure in the buffer and backfill.
3. Displacement of the cansisters in the deposition holes.

### 4.1.1 COMPASS (H.R Thomas and P.J Cleall, Cardiff University)

#### *Basics*

Partly saturated soil is considered as a three-phase porous medium consisting of solid, liquid and gas. The liquid phase is considered to be pore water containing multiple chemical solutes and the gas phase as pore air. A set of coupled governing differential equations can be developed to describe the flow and deformation behaviour of the soil.

The main features of the formulation are:

- Moisture flow considers the flow of liquid and vapour. Liquid flow is assumed to be described by a generalised Darcy's Law. Vapour transfer is represented by a modified Philip and de Vries approach.
- Heat transfer includes conduction, convection and latent heat of vapour transfer in the vaporisation phase.
- Flow of dry air due to the bulk flow of air arising from an air pressure gradient and dissolved air in the liquid phase are considered. The bulk flow of air is again represented by the use of a generalised Darcy's Law. Henry's Law is employed to calculate the quantity of dissolved air and its flow is coupled to the flow of pore liquid.
- Deformation effects are included via either a non-linear elastic state surface approach or an elasto-plastic formulation. In both cases deformation is taken to be dependent on suction, stress and temperature changes.
- Chemical solute transport for multi-chemical species includes diffusion dispersion and accumulation from reactions due to the sorption process.

### *Basis for formulation of governing equations*

Heat conduction and flow are expressed using classical physics but is generalized by including the velocities of liquid, vapour and air respectively. For unsaturated soil the heat capacities of solid particles, liquid, vapour and dry air are considered in addition to the degree of saturation with respect to liquid water.

The velocities of pore liquid and pore air are calculated using a generalised Darcy's law with special respect to the chemical solute concentration gradient and the conductivity of the air phase and the pore air pressure. Also, an osmotic flow term in the liquid velocity is included for representation of liquid flow behaviour found in some highly compacted clays.

Air in partly saturated soil is considered to exist in two forms: bulk air and dissolved air. In this approach the proportion of dry air in the pore liquid is defined using Henry's law.

Where a chemical solute is considered non-reactive and sorption onto the soil surface is ignored, the governing equation for chemical transfer can be expressed in terms of diffusion and dispersion, as derived in primary variable form. The approach has been extended to a multi-chemical species form with a sink term introduced to account for mass accumulation from reactions due to the sorption process. This is then coupled to a geochemical model.

The total strain, $\varepsilon$, is assumed to consist of components due to suction, temperature, chemical and stress changes. This can be given in an incremental form, without loss of generality, as:

$$d\varepsilon = d\varepsilon_{\sigma} + d\varepsilon_{c_s} + d\varepsilon_{s} + d\varepsilon_{T} \qquad (4\text{-}1)$$

where the subscripts $\sigma$, $c_s$, $T$ and $s$ *refer* to net stress, chemical, temperature and suction contributions.

A number of constitutive relationships have been implemented to describe the contributions shown in Eq (1). In particular, for the net stress, temperature and suction contributions both elastic and elasto-plastic formulations have been employed. To describe the contribution of the chemical solute on the stress-strain behaviour of the soil, as a first approximation, an elastic state surface concept was proposed that described the contribution of the chemical solute via an elastic relationship based on osmotic potential theory.

A numerical solution of the governing differential equations presented above is achieved by a combination of the finite element method for the spatial discretisation and a finite difference time stepping scheme for temporal discretisation. The Galerkin weighted residual method is employed to formulate the finite element discretisation. For the flow and stress/strain equations shape functions are used to define approximation polynomials.

### *Software*

The software package, COMPASS, has been developed to implement the numerical approach detailed above. The package has a modular structure to aid the implementation of suitable code and documentation management systems. It has two main components, namely a pre and post processor and an analysis ‘engine’. Evaluation of integrals is achieved via Gaussian integration. For the elasto-plastic based stress equilibrium equations a stress return algorithm is required.

### 4.1.2 CODE_BRIGHT (A. Ledesma, CIMNE, Enresa)

#### *Basics*

A porous medium composed of solid grains, water and gas is considered. Thermal, hydraulic and mechanical aspects are taken into account, including coupling between them in all possible directions. As illustrated in Figure 4-1, the problem is formulated in a multiphase and multi-species approach. The three phases are:

- Solid phase (*s*): minerals
- Liquid phase (*l*): water + air dissolved
- Gas phase (*g*): mixture of dry air and water vapour

The three species are:

- Solid (-): mineral particles
- Water (*w*): as liquid or evaporated in the gas phase
- Air (*a*): dry air, as gas or dissolved in the liquid phase

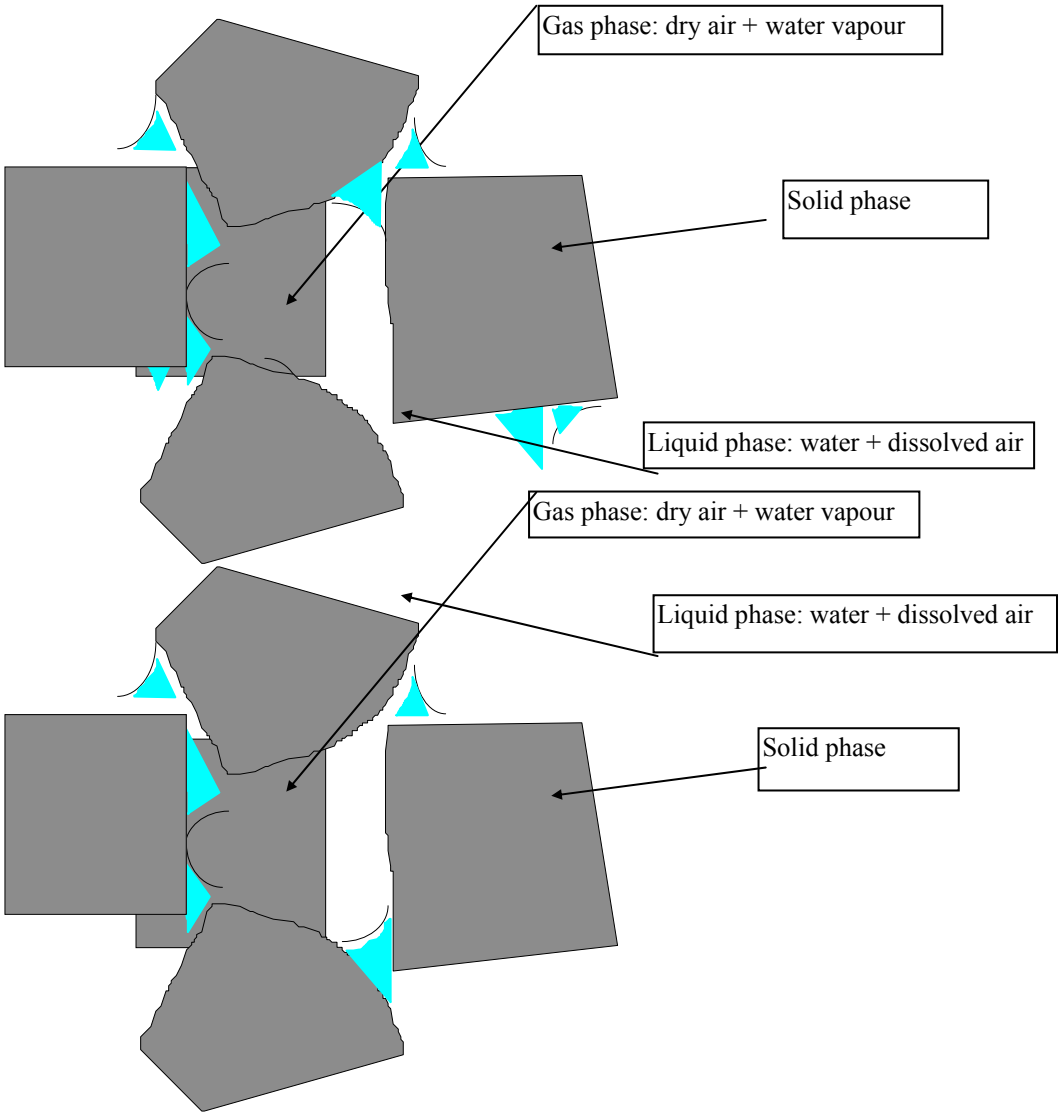


***Figure 4-1.*** *Schematic representation of an unsaturated porous material.*

The following assumptions are considered in the formulation of the problem:

- Dry air is considered a single species and is the main component of the gaseous phase. Henry's law is used to express equilibrium with respect to dissolved air.
- Thermal equilibrium between phases is assumed. This means that the three phases have the same temperature
- Vapour concentration is in equilibrium with the liquid phase, the psychrometric law expresses its concentration.
- State variables (also called unknowns) are: solid displacements, $u$ (three spatial directions); liquid pressure, $P_l$; gas pressure, $P_g$; and temperature, $T$.
- Balance of momentum for the medium as a whole is reduced to the equation of stress equilibrium together with a mechanical constitutive model to relate stresses and strains. Strains are defined in terms of displacements.
- Small strains and small strain rates are assumed for solid deformation. Advective terms due to solid displacement are neglected after transformation of the formulation in terms of material derivatives (material derivatives are approximated as eulerian time derivatives). In this way, volumetric strain is properly considered.
- Balance of momentum for dissolved species and for fluid phases are reduced to constitutive equations (Fick's law and Darcy's law).
- Physical parameters in constitutive laws are functions of pressure and temperature. For example: concentration of vapour under planar surface (in psychrometric law), surface tension (in retention curve), dynamic viscosity (in Darcy's law), are strongly dependent on temperature.

The governing equations that the code solves are:1) *Mass balance of solid, 2) Mass balance of water, 3) Mass balance of air, 4) Momentum balance for the medium, 5) Internal energy balance for the medium*

Associated with this formulation is a set of necessary constitutive and equilibrium laws. Table 4-1 is a summary of the constitutive laws, variables and equilibrium restrictions that have been incorporated in the general formulation. The constitutive equations establish the link between the independent variables (or unknowns) and the dependent ones. There are several categories of dependent variables depending on the complexity with which they are related to the unknowns.

**Table 4-1. Constitutive laws.**

| Equation | Variable Name |
|---|---|
| *Constitutive equations* | |
| Darcy's law | liquid and gas advective flux |
| Fick's law | vapour and air non-advective fluxes |
| Fourier's law | conductive heat flux |
| Retention curve | Liquid phase degree of saturation |
| Mechanical constitutive model | Stress tensor |
| Phase density | liquid density |
| Gases law | gas density |
| *Equilibrium restrictions* | |
| Henry's law | Air dissolved mass fraction |
| Psychrometric law | Vapour mass fraction |

### *Basis for formulation of governing equations*

The resulting system of partial differential equations is solved numerically, dividing the operation into spatial and temporal discretizations. The finite element method is used for the spatial discretization while finite differences are used for the temporal one.

The mechanical stress-strain relationship of the buffer clay is defined by means of an elasto-plastic model specially designed for unsaturated soil and known as the "Barcelona Basic Model". The early difference in physical state between the zone with pellets and the blocks of bentonite is considered by using different parameters but the same model. Rock is taken to be elastic in all the analyses.

A new version of Code_Bright has been recently developed that is able to analyze THMC problems in a coupled manner. The types of processes that can be considered include complex formation, oxidation/reduction reactions, acid/base reactions, precipitation/dissolution of minerals, cation exchange, sorption and radioactive decay. This is in fact a tool that most probably will be used in the future, once all the geochemical information from the experiment has been collected.

### 4.1.3 RF/RM (ROCKFLOW/ROCKMECH, L. Liedtke, BGR)

#### *Basics*

Completely coupled thermo/hydraulic/mechanical models considering the non-linear effects caused by i.a. permeation under unsaturated conditions and the elasto-plastic behaviour of the buffer clay are basic to the RF/RM model. For the buffer one also needs to consider the influence of dessication fractures, swelling and microstructural changes. Major processes in the saturation and subsequent percolation of the buffer are:

- Reduction of the permeable pore space by the expansion of the smectite clay particles and thereby the hydraulic conductivity.
- Changes in effective stress and strain in the saturation phase, which affect the mechanical behaviour of the clay. Here, changes in temperature, water content and stress conditions in both the buffer clay and confining rock play a major role.
- Formation and transport of vapour.
- Osmosis.

The following principles and concepts are basic to the model:

- Effective stress and consolidation concepts (Biot, Terzaghi).
- Mohr-Coulomb failure concept including the influence of internal friction, cohesion, and dilatancy.
- Drucker/Prager's (1952) model of the first invariant of the total stress tensors and the second invariant of stress deviators.
- Roscoe/Schofield/Burland's (1958-1971) Cam-Clay-Model.

#### *Basis for formulation of governing equations*

Four unknown field functions are to be determined: gas pressure $p_g$, water pressure $p_W$, solid displacements, $u$, and equilibrium temperature $T$. In addition to physical changes (stress/strain, drying and wetting) and chemical alteration some of the properties used for modelling, like alteration of the heat conductivity of buffer under saturation, and microstructural changes, have to be taken into consideration.

One can identify impacts in the form of hydromechanical, thermomechanical and hydrothermal effects. For non-isothermal processes in partially saturated porous media it is more convenient to separate dry air and vapour and formulate a mass balance equation for both liquid species, i.e. liquid and liquid vapour.

Concepts for formulations are compositional or phase-related. The first approach consists of balancing the species rather than the phases. The compositional approach is adopted to establish the mass balance equations.

#### *Hydromechanical effects*

Water saturation and swelling of the buffer lead to changes on the microstructural level like changes in porosity, hydraulic conductivity and deformation moduli.

### *Thermomechanical effects*

Temperature-dependent dessication changes the stress/strain behaviour of the buffer clay and causes a need for developing thermo-plastic stress/strain material models and extension of the models describing visco-elastic and visco-plastic strain.

### *Hydrothermal effects*

- The most important hydrothermal effects are related to:
- Redistribution of the initial porewater content in the buffer including vapour formation and condensation.
- Changes in viscosity and hydraulic conductivity of water in different temperature regions.
- Influence on porewater pressure and saturation rate by the groundwater pressure in the rock.
- Alteration of the heat conductivity of buffer under saturation.
- Chemical alteration of the porewater and mineral phases (disregarded so far in the model).

### *Modelling of the Excavation-Disturbed Zone with respect to water uptake and hydraulic pressure distribution in the bentonite buffer*

A model has been developed for predicting the hydration of the initially unsaturated buffer with respect to the interaction with the surrounding rock. The inflowing water from the rock is distributed over the EDZ, which can be supplied with water from discrete water-bearing fractures that intersect the deposition holes. A basic principle of the model is that the hydraulic behaviour of the EBS system is controlled by the saturation of the buffer and vice verse.

The transient groundwater flow in the system is described by:

$$S_0 \frac{\partial h}{\partial t} + \nabla v = q \qquad (4\text{-}2)$$

where $h$ is the piezometric head, $t$ the time, $S_0$ the specific storativity, $v$ the average fluid velocity vector, and $q$ the fluid sink/source.

The velocity is given by the three-dimensional, linear Darcy law:

$$v = -K \cdot \nabla h \qquad (4\text{-}3)$$

where $K$ is the hydraulic conductivity tensor, or by the general form of various non-linear laws for fracture or tubular flow:

The finite element method is used for the numerical simulation of transport and time derivatives, which are evaluated by using different schemes with various orders of accuracy. The stability of numerical solutions depends on the reference point in time of difference formulae. In general, a distinction is made between explicit and implicit schemes. A number of approximate schemes with respect to stability and consistency are examined. The Neumann stability criterion states that the intrinsic values of the amplification matrix of the discretizised equation must be lower or equal to unity. Important stability criteria are stated in terms of the Courant number $Cr$.

### 4.1.4 THAMES (Y. Sugita, JNC)

#### *Basics*

The mathematical formulation for the model utilizes Biot's theory with the Duhamel-Neuman's form of Hooke's law, and an energy balance equation. The governing equations are derived with fully coupled thermal, hydraulic and mechanical processes. They were derived under the following assumptions:

1. The medium is poro-elastic.
2. Darcy's law is valid for the flow of water through a saturated-unsaturated medium.
3. Heat flow occurs in solid and liquid phases (impact of vapor is not considered).
4. Heat transfer among three phases (solid, liquid and gas) is disregarded.
5. Fourier's law holds for heat flux.
6. Water density varies depending upon temperature and the pressure of water

#### *Rheology*

The Terzaghi effective stress principle and Bishop and Blight's extended definitions an equation for saturated and unsaturated media is used:

$$\sigma_{ij} = \sigma'_{ij} + \chi \delta_{ij} \rho_f g \psi \tag{4-4}$$

where $\sigma'_{ij}$ is the effective stress, $\delta_{ij}$ is the Kronecker's delta, $\rho_f$ is the unit weight of water, $g$ is the acceleration of gravity and $\psi$ the pressure head. Subscript $f$ means "fluid". The effects of temperature on the stress/strain behaviour of an isotropic linear elastic material follows the constitutive law:

$$\sigma'_{ij} = C_{ijkl} \varepsilon_{kl} - \beta \delta_{ij} (T - T_o) \tag{4-5}$$

where $\beta = (3\lambda+2\mu)\alpha_T$. $C_{ijkl}$ is the elastic matrix, $\varepsilon_{kl}$ the strain tensor, $T$ the temperature, $\lambda$ and $\mu$ Lamé's constants, and $\alpha_T$ the thermal expansivity coefficient. Subscript $o$ means that the parameter is in a reference state.

#### *Moisture transport*

The equation of porewater motion is expressed by Darcy's law. The physico/chemical state of the gaseous phase in soil is too complicated to be modelled and in the present case pores in the buffer clay are assumed to be filled with only a liquid phase. This means that the ground water does not change in phase from liquid to gas or vice verse and that the thermal conductivity of the gaseous phase is disregarded. Since the heat conductivity of the gaseous phase is smaller than that of the liquid and solid phases, the heat conductivity of the composite material is not affected much by the volume of the gaseous phase.

### *Basis for formulation of governing equations*

The behaviour of the buffer material is influenced by the interdependence of thermal, hydraulic and mechanical phenomena. To treat the water/vapor movement and heat-induced water movement, the continuity equation used in the extended THAMES code contains terms representing the isothermal water diffusivity, the volumetric water content, the water potential head and the intrinsic permeability (*K)*. This equation means that the water flow in the unsaturated zone is expressed by a diffusion term and in the saturated zone by the Darcy's law.

The stress/strain relationship at equilibrium takes the swelling behaviour into account and considers the elastic matrix, the density of the medium and the body force. The effective stress in the unsaturated and saturated zones are functions of the thermal expansion. The swelling pressure is assumed to be a function of the water potential head.

## 4.1.5 ABAQUS (L. Boergesson, Clay Technology AB, SKB)

### *Basics*

The finite element code ABAQUS has been extended to include special material models for rock and soil and ability to model moisture transport associated with stress and strain on various scales. The hydro-mechanical model consists of a porous medium and a wetting fluid and is based on equilibrium, constitutive equations, energy balance and mass conservation using the effective stress theory.

The simplified equation used in ABAQUS for the effective stress is:

$$\overline{\boldsymbol{\sigma}}^{*} = \boldsymbol{\sigma} + \chi\, u_{\mathrm{w}}\mathbf{I}. \qquad (4\text{-}6)$$

where $\boldsymbol{\sigma}$ is the total stress, $u_w$ is the porewater pressure, $\chi$ is a function of the degree of saturation (usual assumption $\chi = S_r$), and $\mathbf{I}$ the unitary matrix.

### *Moisture transport*

Vapour flow is modelled as a diffusion process driven by a temperature gradient. Flow of liquid water is expressed in terms of Darcy's law corrected with respect the degree of water saturation.

### *Coupling of thermal and hydro-mechanical solutions*

In ABAQUS the coupled problem is solved through a "staggered solution technique" as shown in Figure 4-3.

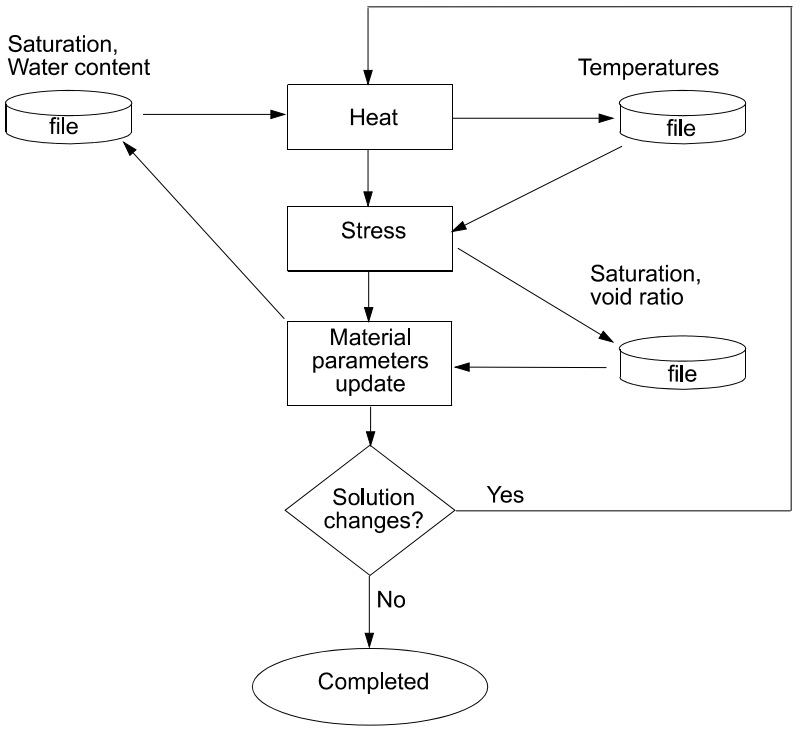


***Figure 4-3.*** *In ABAQUS, heat transfer calculations and hydro-mechanical calculations are decoupled. By using the iteration procedure schematically shown above, the effects of a fully coupled THM model are achieved.*

### *Basis for formulation of governing equations*

*Heat transport*

Thermal flux by conduction is modelled as thermal conduction using the conventional theory with thermal conductivity and specific heat as variables.

*Moisture transport*

The water flux in the liquid phase is modelled by Darcy's law with the water pressure difference as driving force in the same way as for water saturated clay. The magnitude of the hydraulic conductivity $K_p$ of partly saturated clay depends on the void ratio, degree of saturation, and temperature. In the form used here $K_p$ is assumed to be a function of the hydraulic conductivity $K$ of saturated clay and the degree of saturation $S_r$.

Water vapour flow is modelled as a diffusion processes driven by the temperature gradient and the water vapour pressure gradient (under isothermal conditions).

*Hydraulic coupling between the pore water and the pore gas*

The pore pressure $u_w$ of the unsaturated buffer material is always negative and expressed as a function of the degree of saturation $S_r$ independent of the void ratio. ABAQUS also allows for hysteresis effects, which means that two curves may be given (drying and wetting curves).

*Mechanical behaviour of the particle skeleton*

The mechanical behaviour has been modelled using a non-linear Porous Elastic Model and a Drucker-Prager Plasticity model. The effective stress theory as defined by Bishop is applied and adaptated to unsaturated conditions. The shortcoming of the effective stress theory is compensated for by a correction called "moisture swelling" that is a function of the degree of saturation.

*Thermal expansion*

The volume change caused by the thermal expansion of water and particles is modelled but only expansion of the separate phases is taken into account. The possible change in volume of the particle structure by thermal expansion (not caused by expansion of the separate phases) is not modelled. However, a thermal expansion in water volume will change the degree of saturation, which in turn will change the volume of the structure.

## 4.2 Prediction of the evolution of buffer and backfill

### 4.2.1 General

The respective models have been used for predicting the EBS evolution and the most up-to-date results are presented here by the respective modelling groups. For the sake of clarity and simplicity the summation of data was intended to concern only the "wettest" hole (No 1) but it was extended to cover also Hole 3 by two of the modellers.

### 4.2.2 Predictions for comparison with actual recordings

The work presented here has comprised 3D or axisymmetric hydraulic analyses of the temperature evolution, hydration and build-up of swelling pressure in the buffer assuming unlimited access to water from the rock, which corresponds to the conditions in the wettest deposition hole at AEspoe.

The geometry of the model for 3D FEM calculations is shown in Figure 4-4. Special definitions respecting the considered holes and boundary conditions are specified by the respective modeling group.

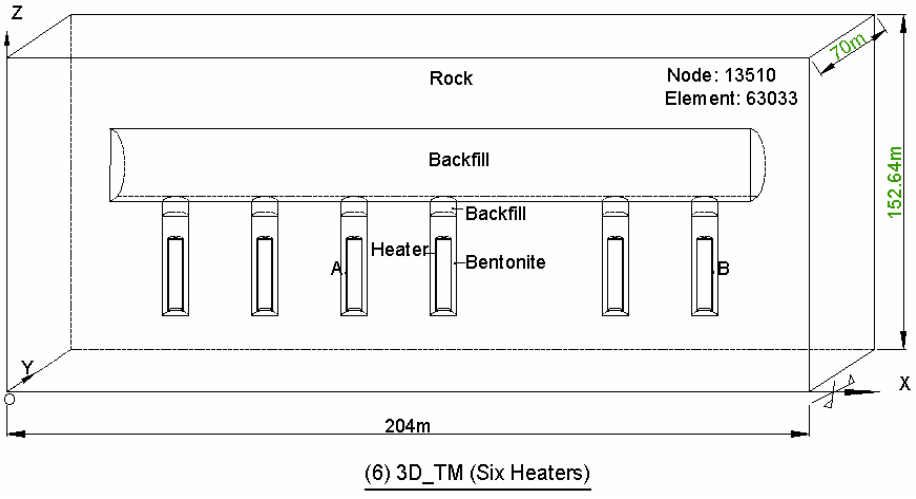


***Figure 4-4.*** *Schematic view of generalized 3D model.*

The calculations have been based on the following data:

- Material data provided by SKB
- The initial temperature throughout the domain set at 12-14$^{o}$C.
- The heat generation of the electric power taken as 1800 W.

### 4.2.3 COMPASS (H.R Thomas, P.J Cleall, T.A. Melhuish, University of Cardiff)

#### *General*

A full three-dimensional model of the Prototype Repository incorporating all of the primary features of the tunnel has been developed. The model domain measures 200 m by 100 m by 200 m and is shown in Figure 4-5a. This model has been discretizised using 8 noded hexahedral elements and consists of 158,175 elements and 146,380 nodes and is shown in Figure 4-5b. The mesh has been refined in and around the buffer with a coarser mesh discretization of the far-field rock. The size of the model has been reduced by 50% via the introduction of a vertical symmetry plane along the centre of the tunnel by which the computational requirements of the model were considerably reduced. This geometrical model has been used for the majority of the numerical modelling work with smaller three-dimensional and two-dimensional models being implemented to investigate the mechanical response of the buffer and pellets under thermal and hydraulic gradients.

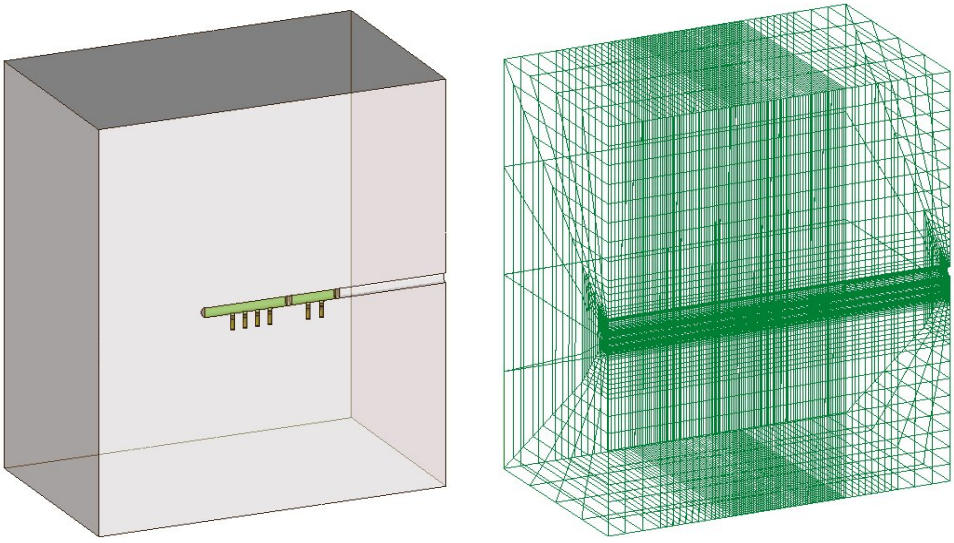

***Figure 4- 5a****: 3D tunnel domain* ***4-5b****): 3D tunnel mesh*

A large number of coupled thermal-hydraulic-mechanical analyses have been performed to investigate the complex flow patterns that occur in the Prototype Repository following heater activation. In order to establish an understanding of these processes a comprehensive step-wise approach to the modelling has been adopted. A full range of 3D tunnel section and 2D axisymmetric analyses have been undertaken with the results being presented previously [4-1]. However, more recently a full three-dimensional, analysis of Section I has been performed. Recent research has shown that the micro and

macro structure of a bentonite buffer material may have a pronounced effect on the saturation rates of the material [4-2]. It was proposed that as water enters the buffer the majority of it becomes adsorbed within the micropores and hence becoming unavailable for further flow. Depending on the degree of mechanical restraint, swelling of the micropore will lead to some reduction in the size of the macropores [4-3]. As the only water available for flow is contained in the macropores, the swelling of the micropores in a restrained material would thus tend to 'choke' moisture flow and further reduce the effective hydraulic conductivity of the material. Following the approach presented in [4-2] the hydraulic conductivity relationship used here has been modified accordingly.

### *Temperature at mid-height canister*

The power adopted in the coupled thermal-hydraulic-mechanical analyses has been taken from the recorded power of Canister 1 as detailed in the Appendix. This approximates to a constant power of 1800 W in the first year and then a gradual reduction of 20 W per year thereafter. Figure 4-6 shows both the simulated and experimentally measured temperature plots after 900 days for the 3 different radii positions in Hole 1 at the mid-height of the canister. It can be seen that there is excellent agreement between the sets of results. At a radius of 0.585 m the temperature has been simulated to be 71.5 ºC after 717 days. The corresponding experimentally measured value at the same position is 71.4 ºC. At a radius of 0.685 m the temperature is simulated as 64.8 ºC after 717 days, with a corresponding experimentally measured value of 65 ºC. Finally, at a radius of 0.785 m, there were no results measured after approximately 550 days when the temperature was recorded to be 58.2 ºC. The simulated value at the same position and similar time was 58.3 ºC. These results illustrate that the temperature regime is well understood and captured by the model in Hole 1.

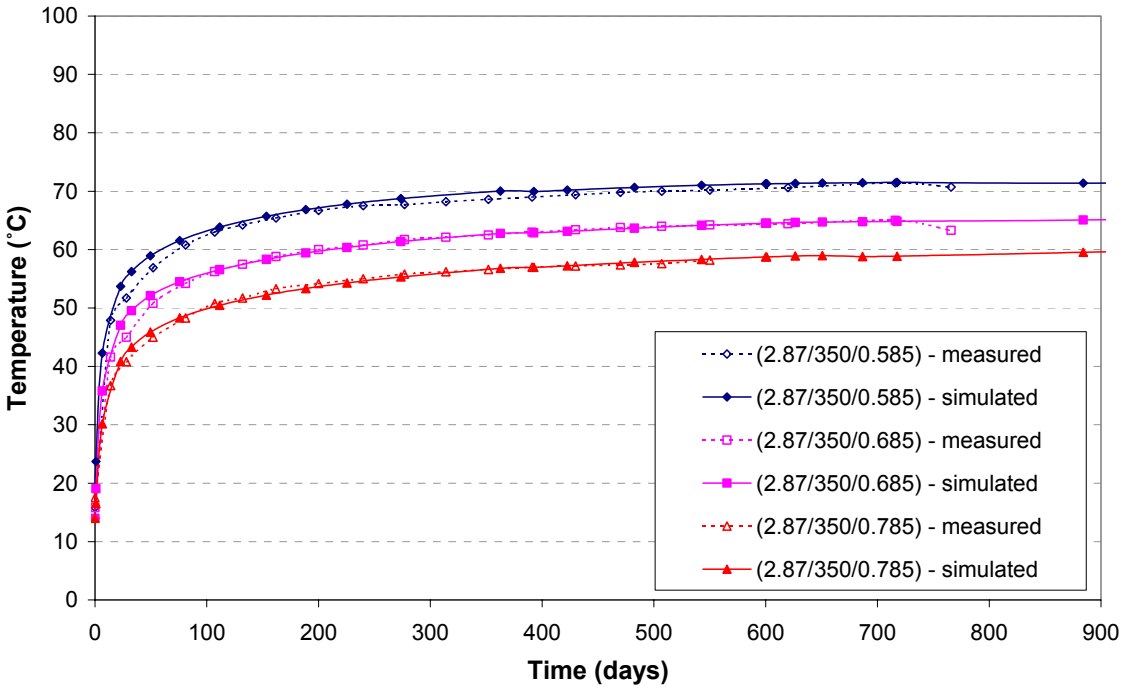


***Figure 4-6.*** *Measured and simulated temperature plots for Hole 1/Ring 5. Legend numbers 0.585, 0.685 and 0.785 m point out the distance from the centre of the deposition hole. The radius of the canister is 0.525 m and of the deposition hole 0.875 m.*

### *Hydration of buffer at mid-height canister*

In order to capture the rate of re-saturation of the buffer in Hole 1 it is critical to accurately model the supply of water from the granite rock including any water bearing fractures. Based on the simulated inflow rates into Hole 1 as detailed in previous work [4-1] the hydraulic conductivity of the granite was assumed to be $10^{-11}$ m/s with a representative fracture intersecting the borehole with a hydraulic conductivity of $10^{-9}$ m/s. Figure 4-7 shows the simulated and experimentally measured degree of saturation plots for 3 different radii positions in Hole 1 at the mid-height of the canister. It can be seen that initially there is an over-prediction of drying in the buffer. At a radius of 0.785 m a minimum value of 78.6 % is reached after approximately 20 days. Experimentally, the buffer closest to the rock exhibits immediate recharge following heater activation with the pellet filled region appearing to have very little effect in terms of retarding the rate of re-saturation in the more centrally located buffer. After 100 days the correlation between the experimental and simulated results is much improved, with almost complete saturation being achieved after approximately 400 days in both cases.

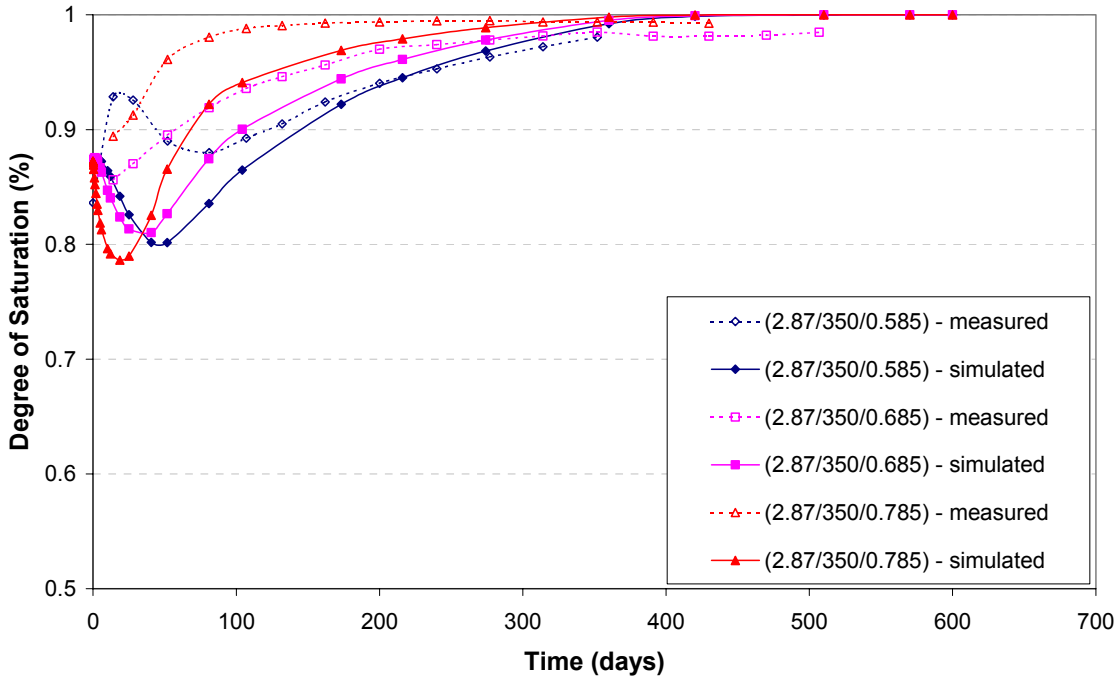


***Figure 4-7.*** *Measured and simulated degree of saturation plots for Hole 1/Ring 5. Legend numbers 0.585, 0.685 and 0.785 m point out the distance from the centre of the deposition hole. The radius of the canister is 0.525 m and of the deposition hole 0.875 m.*

### *Total pressure in buffer*

Figure 4-8 shows both the simulated and experimentally measured total pressure plots in the buffer at 4 different positions in Hole 1. There is good qualitative correlation between the results and quantitatively the simulation has captured the development of swelling pressures in the buffer well except close to the rock/ buffer interface, where the buffer experiences the highest swelling pressure by recharge from the granite. Closest to the canister surface the swelling pressure was simulated as reaching 3.2 MPa compared to a measured pressure of 4.1 MPa after 700 days. At the location closest to the rock/buffer interface the simulated pressure of 3.9 MPa can be compared with the experimentally measured value of 6.7 MPa. It is believed that this difference is due to an overestimation of the compressibility of the pellet region leading to a relief of some of the swelling pressure developed on saturation.

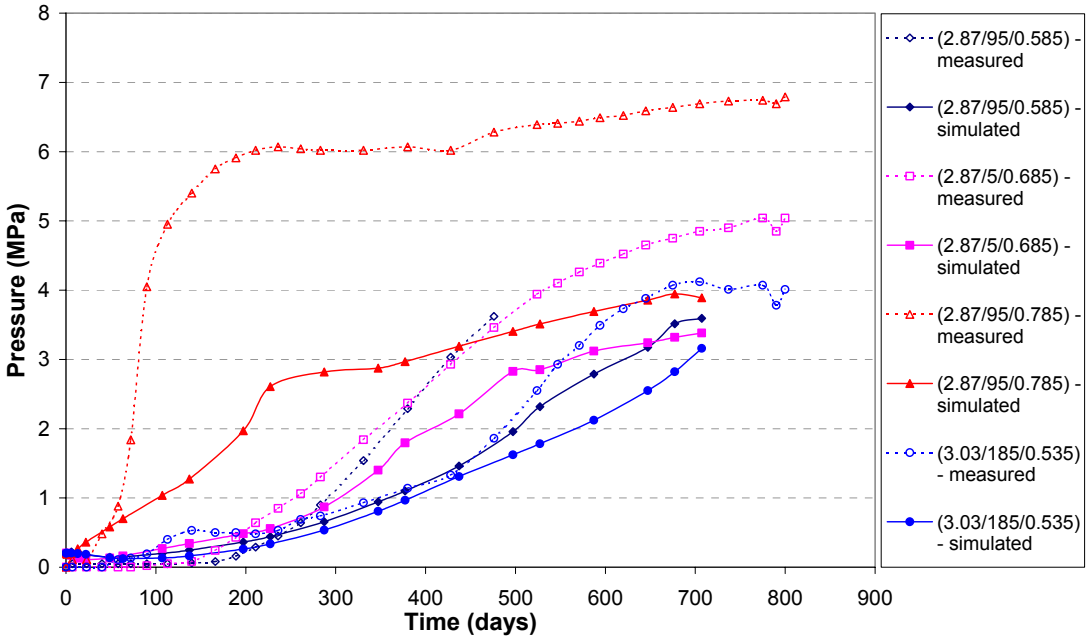


***Figure 4-8.*** *Measured and simulated total pressure plots for Hole 1/Ring 5. Legend numbers 0.585, 0.685 and 0.785 m point out the distance from the centre of the deposition hole. The radius of the canister is 0.525 m and of the deposition hole 0.875 m.*

### *Comparison with Hole 3*

While Hole 1 can be taken as "wet" all other deposition holes in the Prototype Repository test drift have very little inflow of water and probably represent the majority of deposition holes in a repository constructed in crystalline rock. The theoretical UWC-derived and actual evolution of temperature, hydration and total pressure are therefore described here. For space reasons the presentation is given in condensed form.

### *Temperature*

Figure 4-9 shows temperature plots after 624 days for 3 different radii positions in Hole 3. At r=0.585 m the temperature has been simulated to be 76.1 ºC after 624 days, and at r=0.785 m as 68.6 ºC. The measured results are 77.1 ºC and 67.2 ºC respectively. Again, these results illustrate that the temperature regime is well understood and captured by the simulation.

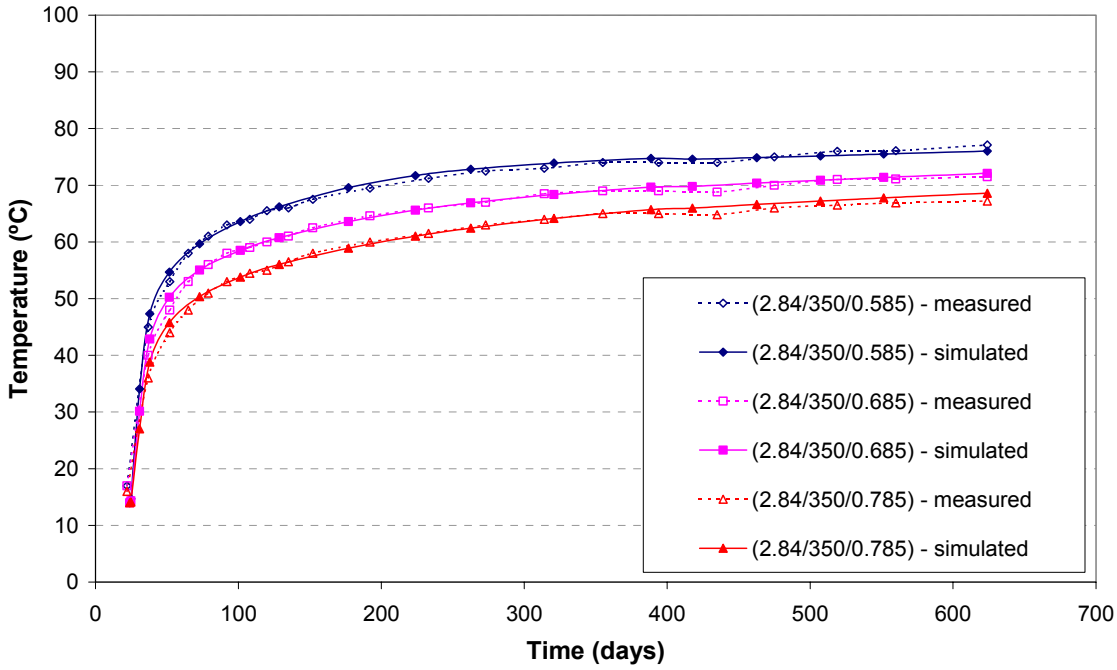


***Figure 4-9.*** *Measured and simulated temperature plots for Borehole 3/Ring 5. Legend numbers 0.585, 0.685 and 0.785 m point out the distance from the centre of the deposition hole. The radius of the canister is 0.525 m and of the deposition hole 0.875 m.*

### *Hydration*

Figure 4-10 shows a comparison between simulated and measured degree of saturation for three different positions in the buffer in Hole 3/Ring 5. Initially there is a decrease in saturation throughout the buffer for both the simulated and measured results as the temperature rises. Drying takes place in the buffer as a consequence of the movement of vapour away from the hotter regions closest to the heater. At r=0.585 m the predicted degree of saturation reaches a minimum of 71.8 % after 225 days and hence follows the measured trends with minimum degree of saturation of 70.4 % after 230 days. In both cases re-saturation begins to take place slowly at a similar rate. This behaviour can also be seen at r=0.685 m for both the simulated and measured results, but with less overall drying taking place due to the larger distance to the heater. At r=0.785 m there is an initial over-prediction of drying that may be a result of an overestimation of suction in the nearby pellet region. However, as this region begins to re-saturate the simulation matches the measured behaviour. Overall, the correlation between the experimental and numerical results is encouraging.

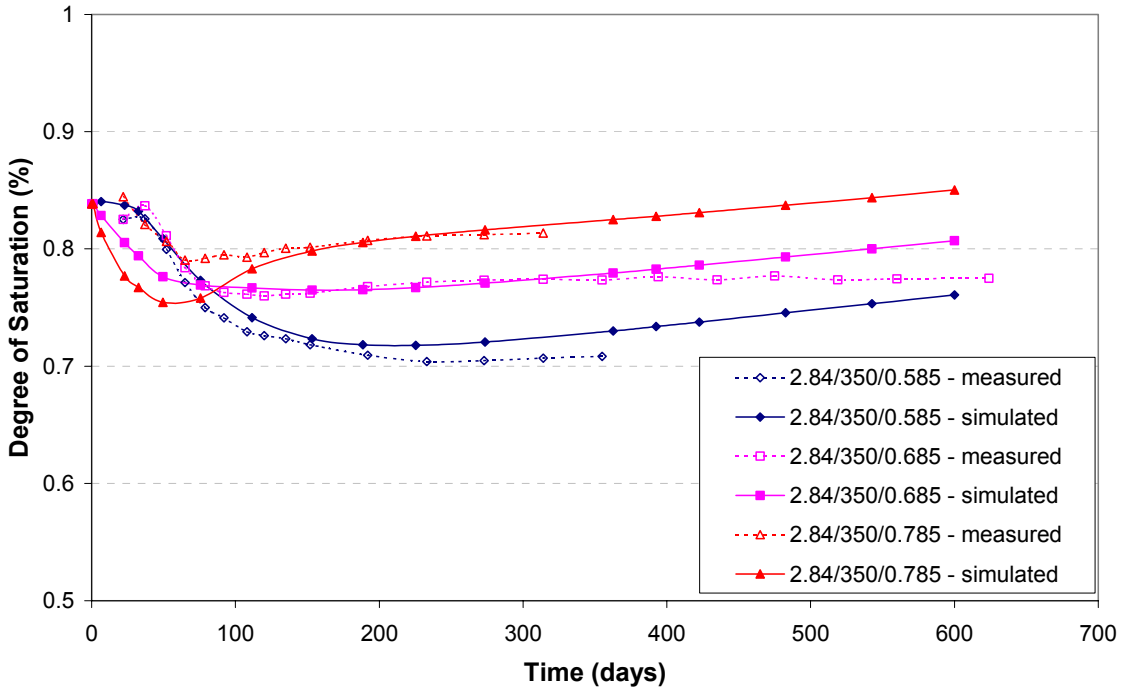


***Figure 4-10.*** *Measured and simulated degree of saturation plots for Hole 3/Ring 5. Legend numbers 0.585, 0.685 and 0.785 m point out the distance from the centre of the deposition hole. The radius of the canister is 0.525 m and of the deposition hole 0.875 m.*

### *Total pressure*

Figure 4-11 shows the simulated and measured total pressure plots in the buffer at 3 different positions in Hole 3. It can be seen that very little swelling pressure develops in the first 600 days and that there is no major change from the initial conditions. These patterns follow the slow rate of re-saturation in the buffer as illustrated in Figure 4-10. It is expected that as the buffer in Hole 3 further re-saturates the swelling pressures will increase accordingly.

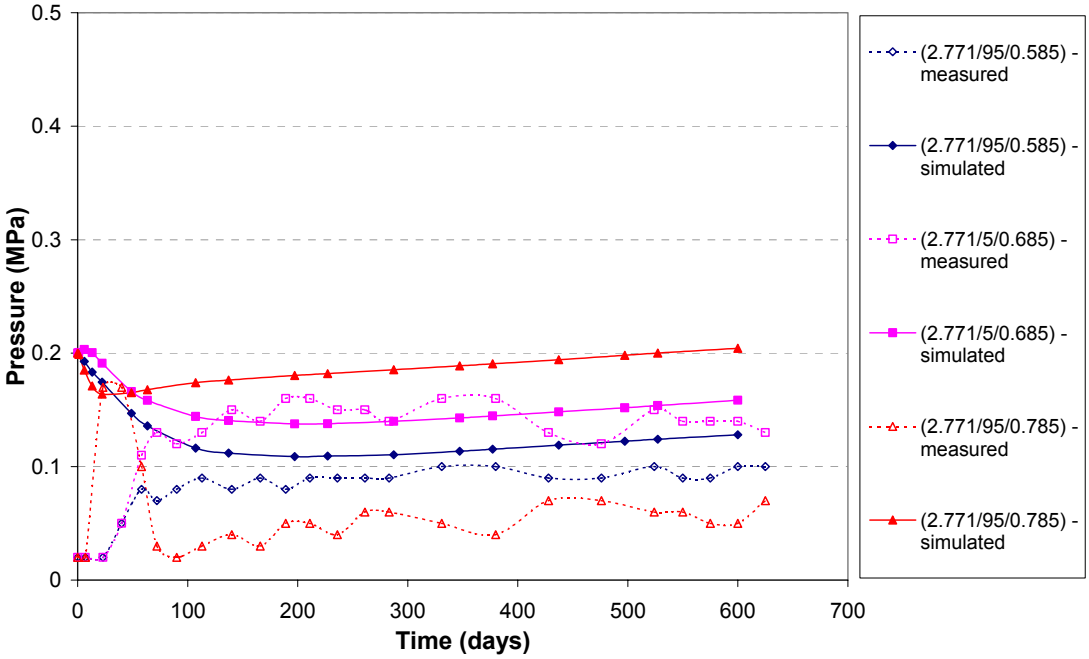


***Figure 4-11.*** *Measured and simulated total pressure plots for Hole 3/Ring 5. Legend numbers 0.585, 0.685 and 0.785 m point out the distance from the centre of the deposition hole. The radius of the canister is 0.525 m and of the deposition hole 0.875 m.*

### 4.2.4 CODE_BRIGHT (A. Ledesma, G.J. Chen, CIMNE, Enresa)

#### *Temperature at mid-height canister*

Different geometries were used to analyze the thermal problem and finally, a fully 3D geometry was considered. When the analysis was coupled with the hydraulic and the mechanical problem, quasi 3D (axisymmetric) conditions were used, in order to avoid large computing times. The results in terms of temperature distribution were not too different except for some 3D effects due to the interaction between canisters, which can be taken into account using appropriate boundary conditions. Figure 4-12 presents a summary of the numerical results, including the evolution of temperature for three typical points of the buffer [4-4,4-5].

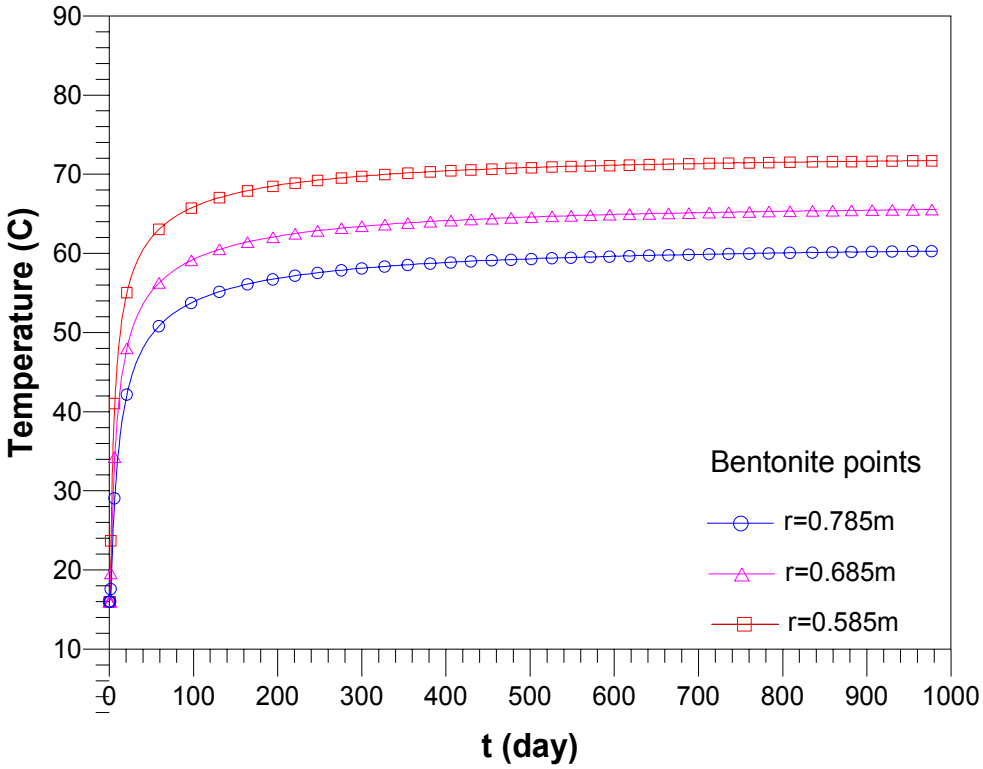


***Figure 4-12.*** *Evolution of temperature computed for three points in the buffer. Legend numbers 0.585, 0.685 and 0.785 m point out the distance from the centre of the deposition hole. The radius of the canister is 0.525 m and of the deposition hole 0.875 m.*

### *Hydration of buffer at mid-height canister*

Figure 4-13 presents the evolution of degree of saturation against time for the mid plane of hole number 1. It should be pointed out that the parameters used in the analyses were the same for all deposition holes, except for the initial boundary conditions (i.e. Hole no 1 was initially wet, whereas Hole no 3 was initially dry). This approach only gives an average prediction and a better fit would have been achieved by using different parameters for each deposition hole. According to the calculations the saturation will be practically complete (99%) after 1000 days in a point close to the rock in Hole 1.

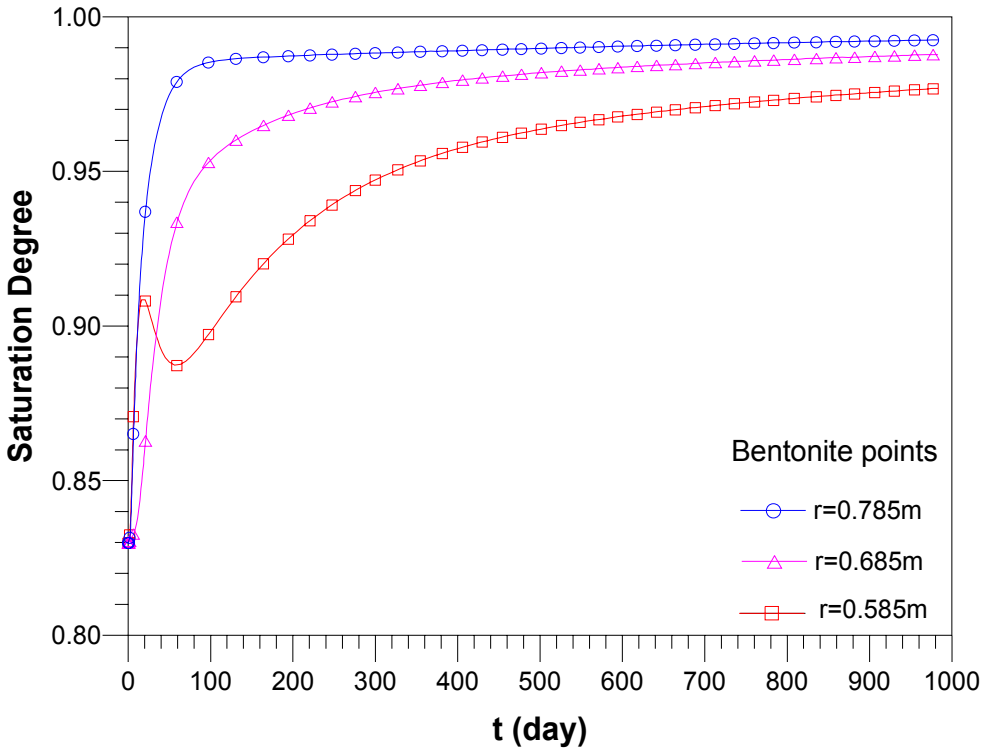


***Figure 4-13.*** *Predicted degree of saturation at mid-height of the heater in Hole 1 (the wettest one). Legend numbers 0.585, 0.685 and 0.785 m point out the distance from the centre of the deposition hole. The radius of the canister is 0.525 m and of the deposition hole 0.875 m.*

### *Total pressure in buffer*

A summary of the analyses is presented in Figure 4-14. It can be seen that after 600 days a pressure of almost 7 MPa is achieved in a point close to the rock, where the saturation runs fast. Points close to the heater reach 4.2 MPa after 600 days. Comparison of this variable with measurements is more difficult than in previous cases (i.e. temperature or saturation degree), due to the limited reliability of the instrumentation recording total pressures. Considering this difficulty the predictions seem reasonable.

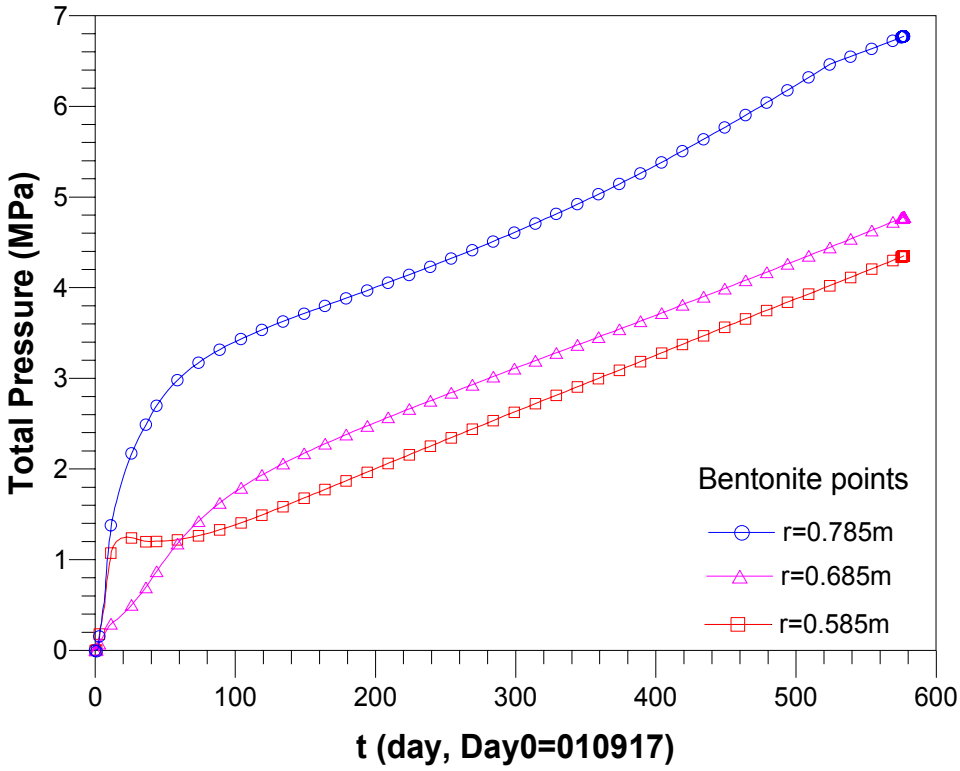


***Figure 4-14.*** *Computed evolution of total pressure for three points. Legend numbers 0.585, 0.685 and 0.785 m point out the distance from the centre of the deposition hole. The radius of the canister is 0.525 m and of the deposition hole 0.875 m.*

### 4.2.5 THAMES (Y. Sugita, JNC)

#### *Temperature at mid-height canister*

A constant heat power of 1800 W was applied to the each heater. As the boundary conditions, temperature was fixed on the top and the bottom surface, and no heat flux was applied to the side surface. Figure 4-15 shows the predicted temperature evolutions at the expected points. The temperature steadily increases with time and does not reach steady state conditions even after 1000 days.

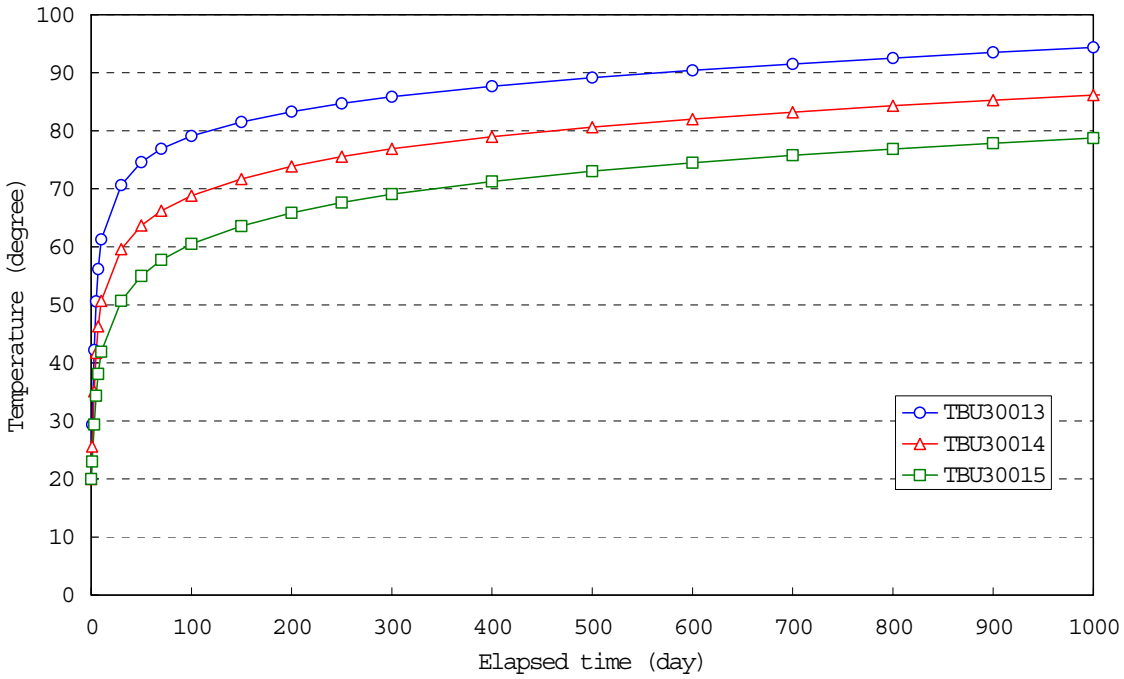


***Figure 4-15.*** *Predicted temperature (3D analysis). The blue, upper curve represents the vicinity of the canister and the green, lowest curve the rock/buffer contact.*

### *Hydration of buffer at mid-height canister*

Initial water content of 17 % for the buffer represents the degree of saturation of approximately 60 %, and the relative humidity of about 80 %. The evolution of the relative humidity and the degree of saturation are shown in Figure 4-16 and 4-17. The relative humidity at each point steadily increases and reaches saturation around 700 days. No drying of the hottest part of the buffer can be expected according to the simulation.

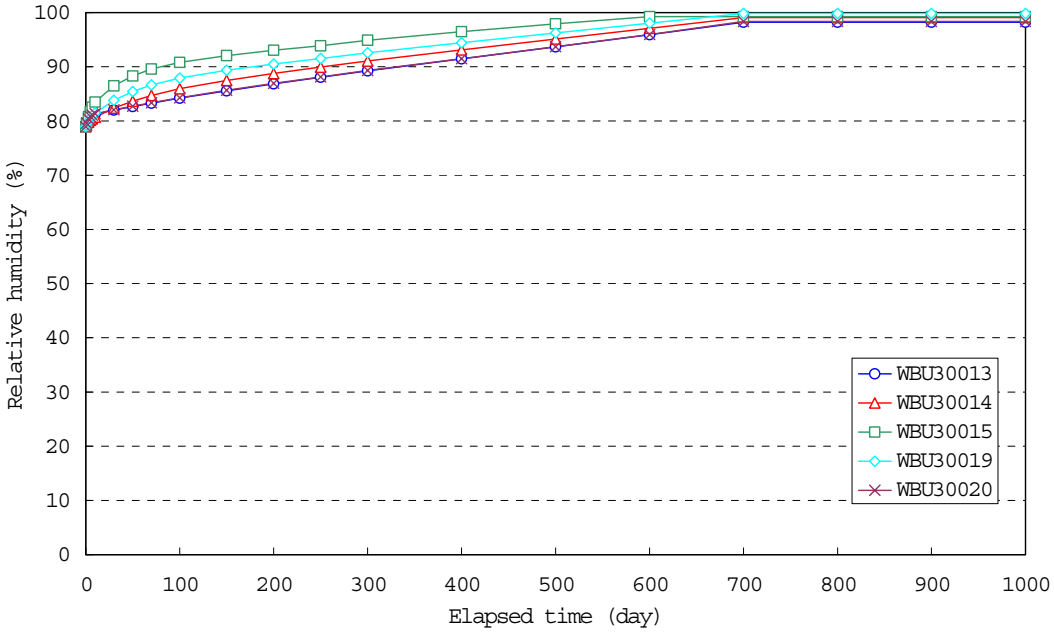


***Figure 4-16.*** *Predicted relative humidity (3D analysis). The blue, lower curve represents the vicinity of the canister and the green, upper curve the rock/buffer contact.*

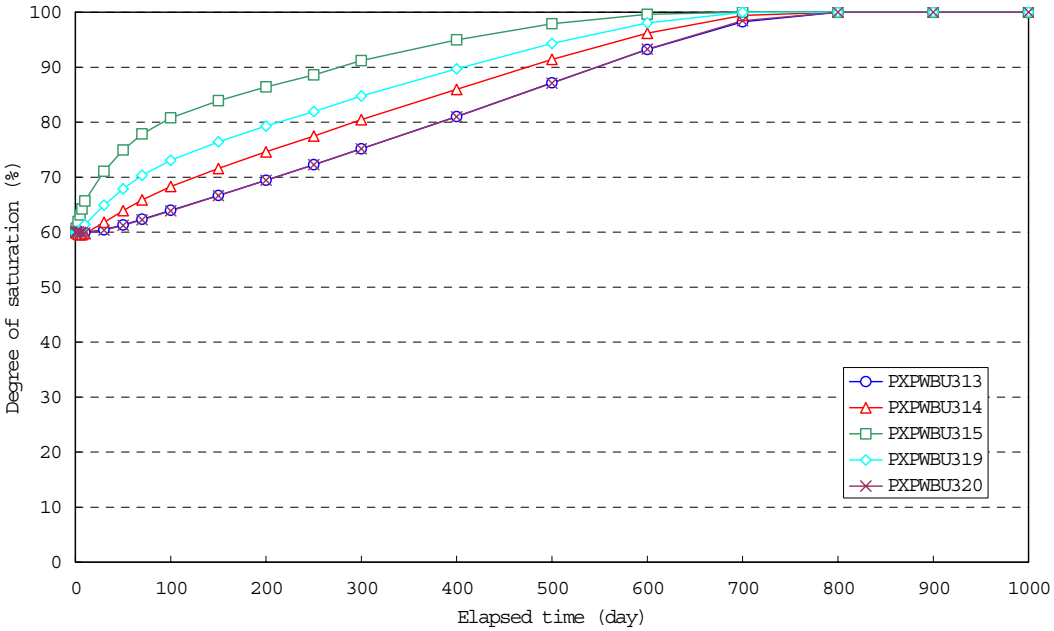


***Figure 4-17.*** *Predicted degree of saturation (3D analysis). The blue, lowest curve represents the vicinity of the canister and the green, upper curve the rock/buffer contact.*

### *Total pressure in buffer*

Figure 4-18 gives the evolutions of the total stress at the selected points. The main contribution to the stress increment is the swelling pressure of the buffer. Therefore, the stress increases with respect to the evolutions of relative humidity (see Figure 4-16).

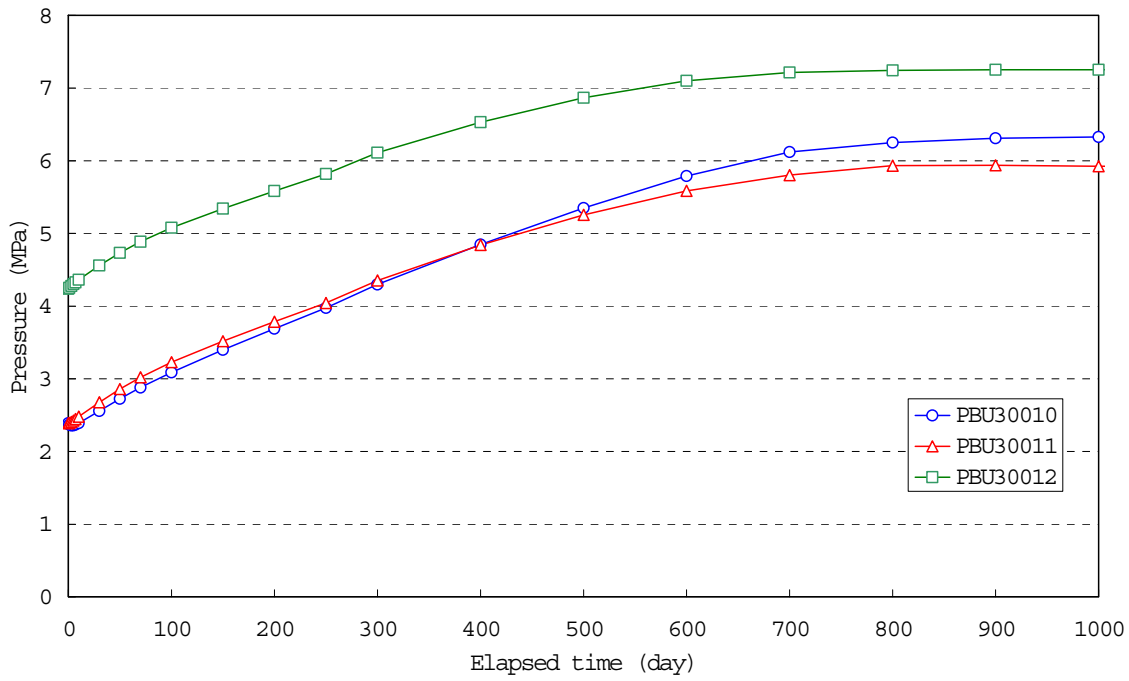


***Figure 4-18.*** *Predicted total stress (3D analysis). The blue lowest curve represents the vicinity of the canister and the green, upper curve the rock/buffer contact.*

### 4.2.6 RF/RM ( L. Liedtke, BGR)

The saturation and resulting swelling pressure of a deposition hole and tunnel system filled with bentonite has been calculated applying two phase flow theory and considering the excavation disturbed zone (EDZ), [4-6,4-7,4-8,4-9].

The work presented here has comprised 3D hydraulic analyses of the temperature evolution, hydration and build-up of swelling pressure in the buffer assuming unlimited access to water from the rock, which corresponds to the conditions in the wet deposition Hole 1 at AEspoe.

The geometry of the model for 3D FEM calculations is shown in Figure 4-19.

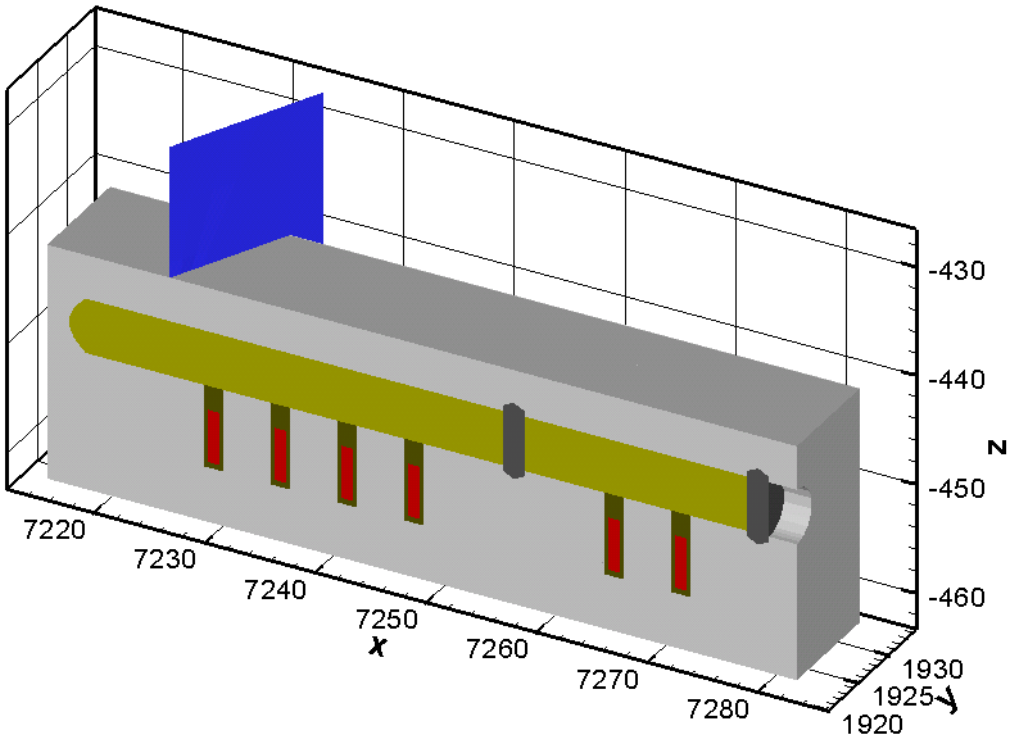


***Figure 4-19.*** *Schematic view of generalized 3D model.*

#### *Temperature at mid-height canister*

Figure 4-20 shows the heat evolution at mid-height of Hole 1. The initial temperature was taken as 18 $^{o}$C and the temperature at the surface of the canister was set at 100 $^{o}$C after 100 days.

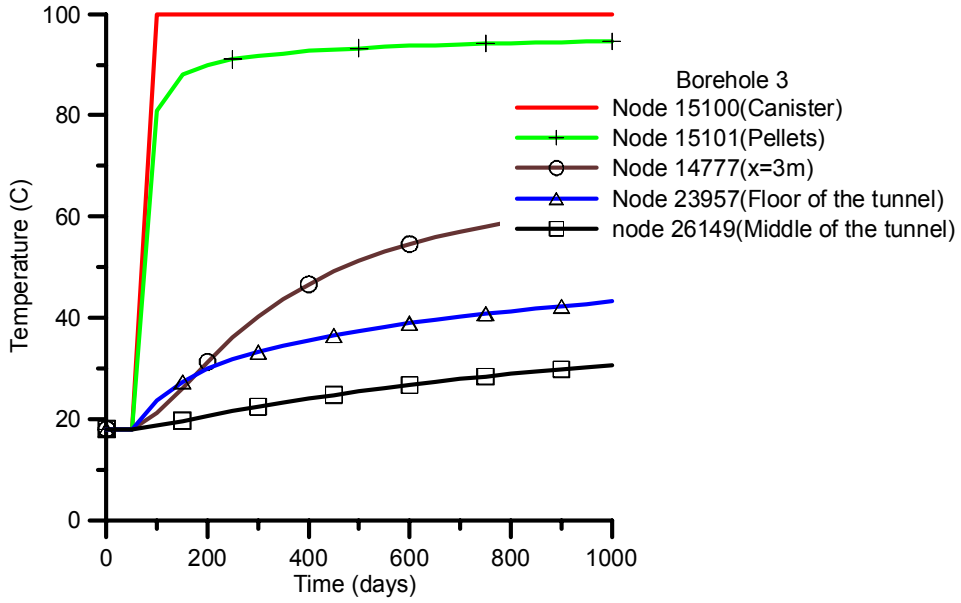


***Figure 4-20.*** *Temperature on the canister surface at mid-height predicted by 3D calculation. A maximum temperature of 100 °C at the canister surface was set by the modeller for the time 100 days.*

### *Hydration and consequent stress evolution*

Figure 4-21 shows the pressure evolution at the upper end of Hole 1 including the effect of upward movement of the canister. The maximum pressure at the canister surface (red curve) proceeds beyond 5 MPa after 3 years.

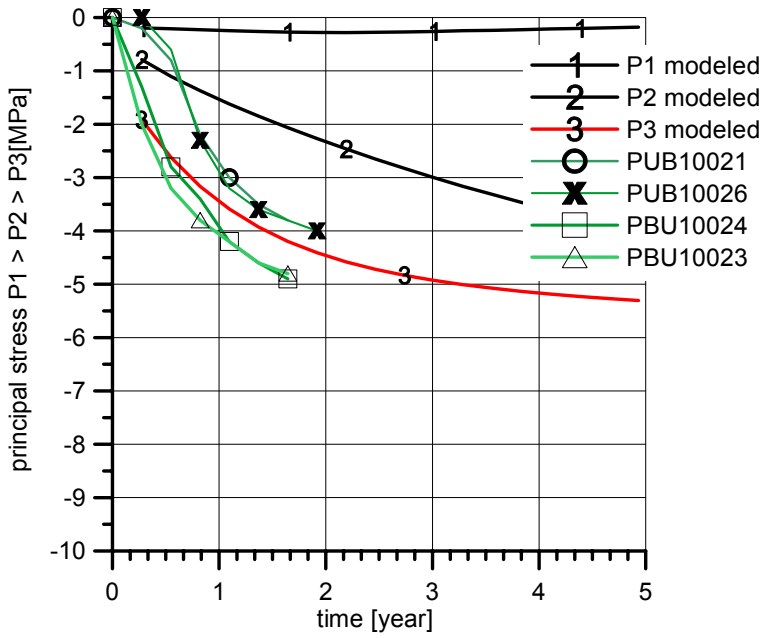


***Figure 4-21.*** *Pressure evolution at the upper end of Hole 1 including the effect of upward movement of the canister (negative pressures represent compressive stresses). After 1 year the predicted pressure at the canister surface is 3.5 MPa and reaches 4.5 MPa after 2 years. At the rock/buffer contact the predicted pressure is about 5 MPa after 1.75 years (green curve).*

### 4.2.7 ABAQUS (L. Boergesson, Clay Technology, SKB)

A constant power of 1050 W was assumed in the calculation, which was based on 75 °C as constant temperature of the (metal) canister surface. It gave a maximum temperature in the buffer close to the canister surface after 2 years ($6x10^7$ s) of about 60 °C and 45 °C at the rock implying an average temperature gradient across the 35 cm thick buffer of 0.42 centigrades per cm radial distance as can be inferred from Figure 4-22. Converting this to the actual 1800 W in the test and assuming the initial temperature to be 10 °C, the temperature in the buffer adjacent to the canister would be about 67 °C and 44 °C at the rock surface after 1 year, and 70 and 47 °C, respectively, after 2 years.

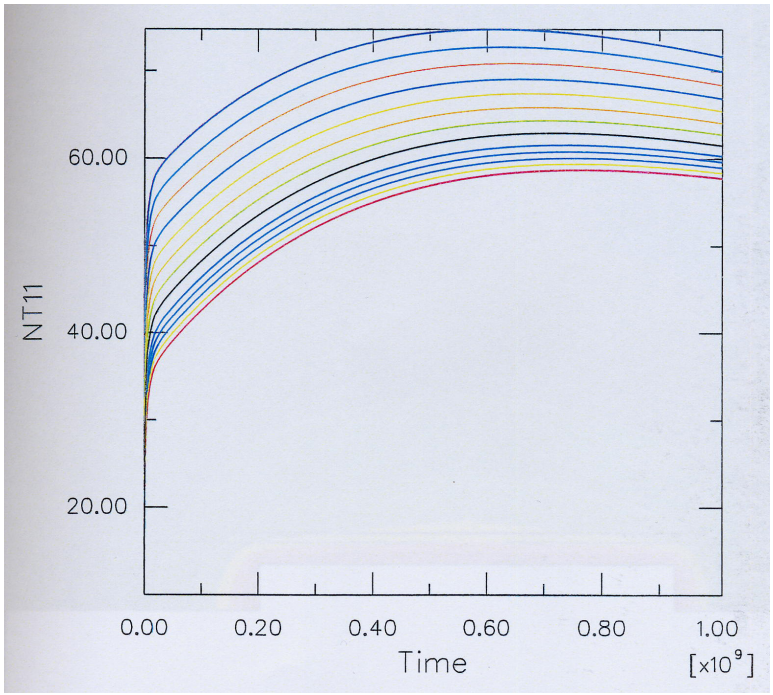


***Figure 4-22.*** *Predicted temperature evolution in the clay at mid-height of the canister in the wettest hole for the first 32 years including 10 °C initial rock temperature surface (1050 W power). The curves represent 13 equally spaced distances from the rock surface (The upper curve is the canister surface and the lower is the rock boundary).*

### *Hydration of buffer at mid-height canister*

The calculation is made for the simplified case with the intial density, which is different for the pellet filling and buffer blocks and gaps in practice, smeared out over the entire volume. It is derived from Figure 4-23 that complete saturation is reached after around 3 years ($10^8$ s).

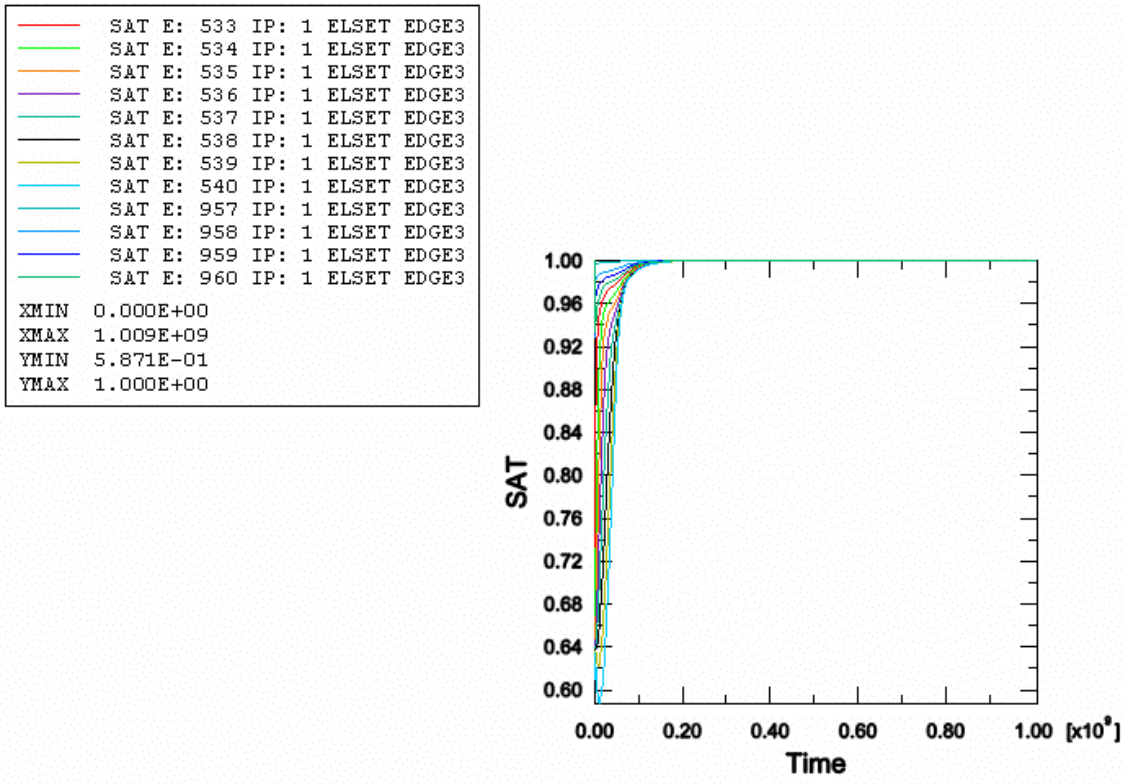


***Figure 4-23.*** *Predicted degree of saturation at mid-height canister in the wettest deposition hole. The curves represent equally spaced distances from the rock surface (Blue is the rock boundary, the curve to the right is the canister surface). Complete saturation of the entire buffer is reached after about 3 years.*

### *Total pressure in buffer*

The calculation shows that full swelling pressure (about 8.5 MPa) will be reached after about 3 years nearly irrespective of the distance from the rock (Figure 4-24). No external water pressure was assumed and the values therefore represent the total pressure.

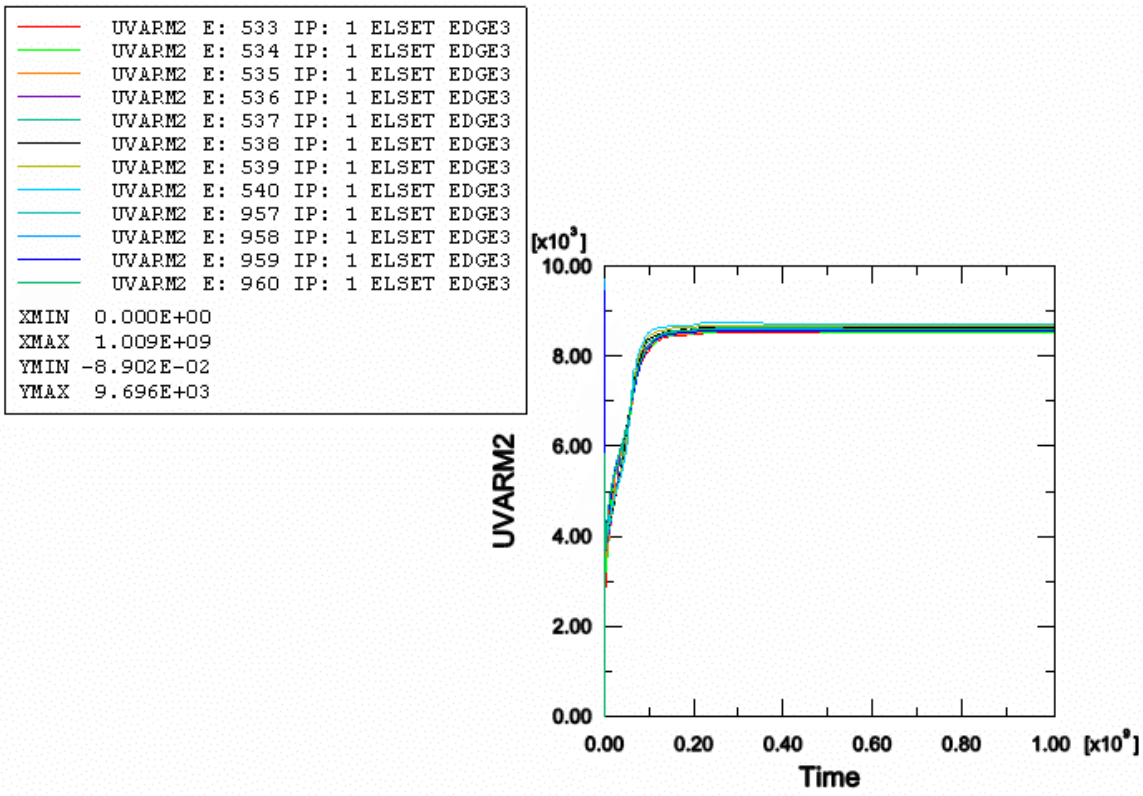


***Figure 4-24.*** *Predicted total pressure at mid-height canister in the wettest deposition hole. No external pressure is assumed and the data therefore represent the swelling pressure as well. The curves represent equally spaced distances from the rock surface (Blue is the rock boundary). The pressure is about 8.3 MPa in the entire buffer after about 3 years.*

## 4.3 Recordings

### 4.3.1 Temperature at mid-height canister in the wettest hole (No 1)

The temperature is still rising after more than 2 years. It reached about 72 $^{o}$C in the clay adjacent to the canister surface and around 60 $^{o}$C at the rock after about 700 days, or around 2 years as shown by Figure 4-25. The average temperature gradient is about 0.34 centigrades per centimetre radial distance. Almost the same temperature figures were also given by the Vaisala RH meters as shown below. The power has been about 1800 W, see Appendix 1.

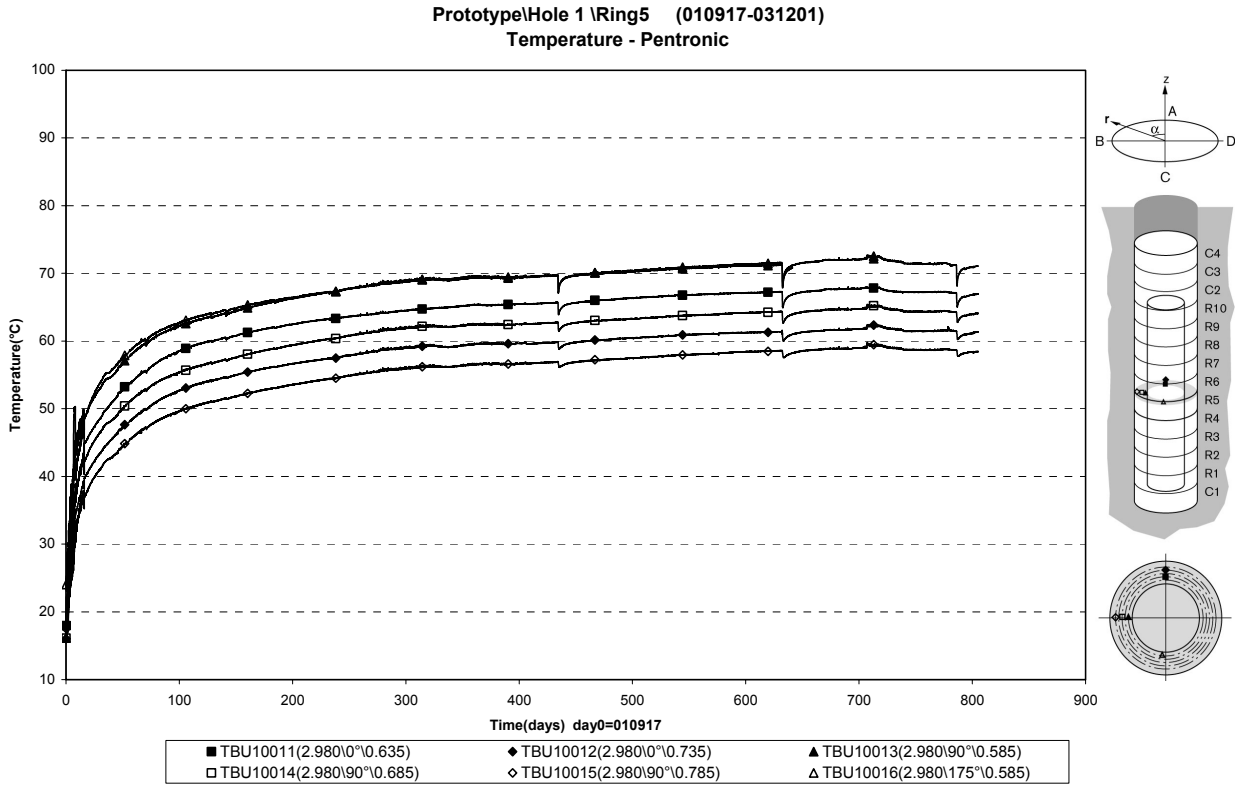


***Figure 4-25.*** *Temperature at mid-height of the canister in the wettest hole (Hole 1). The legend denotes which instrument and where it is located; example TBU10011 (2.980\0$^{o}$\0.635) where TBU is gauge type (here temperature sensor), 10011 is the gauge number, 2.980 is the distance from the hole bottom, 0$^{o}$ is the coordinate angle from the drift axis (see top figure at right), and 0.635 is the distance from hole centre.*

### 4.3.2 Hydration at mid-height canister in the wettest hole (No 1)

The hydration process can be interpreted from the output of the Vaisala RH meters. The results are shown in Figure 4-26 (Recordings), which indicate that the clay had reached RH values of 92-94 % after about one year. It has been assumed that for high RH the values are approximately equal to the degree of water saturation, which should indicate that a very high degree of water saturation had been reached in all parts of the buffer already at this stage. This assumption may have to be reconsidered.

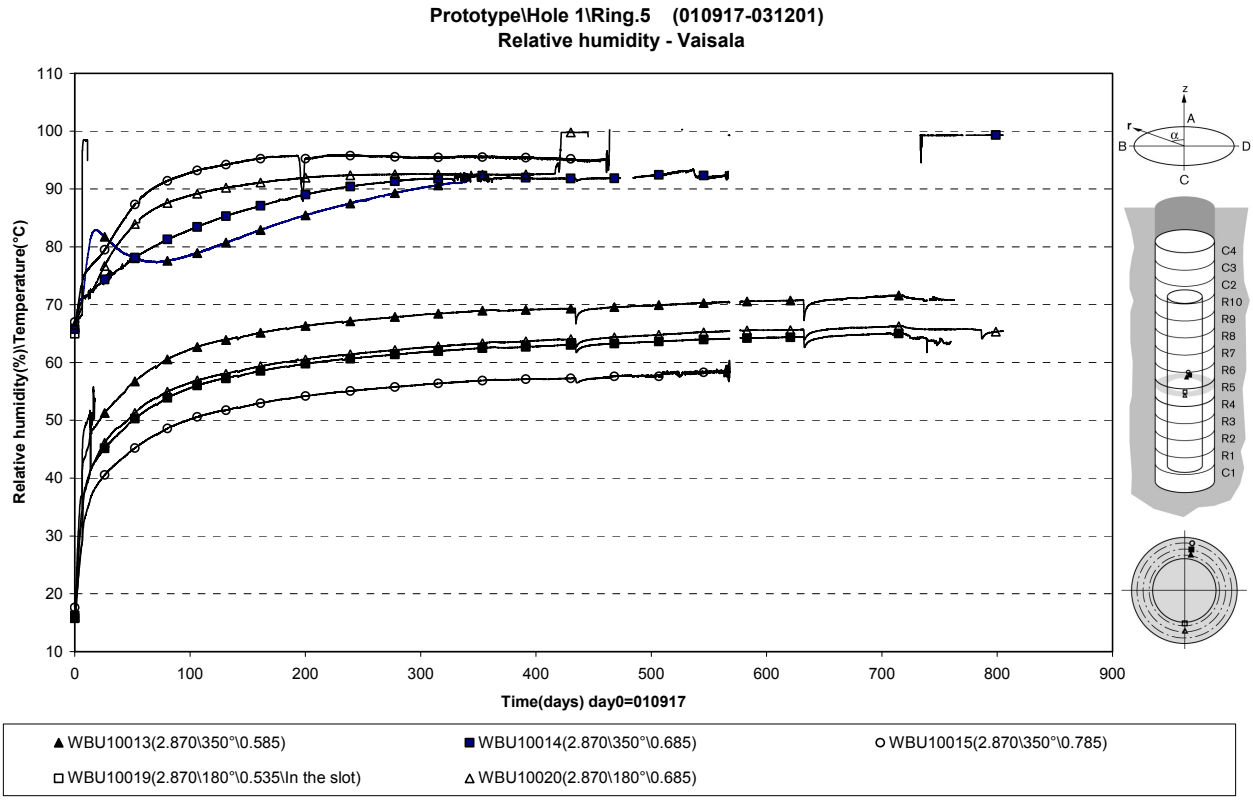


***Figure 4-26.*** *RH and temperature distributions in the buffer in the wettest hole (No 1). The legend is explained under Figure 4-25. WBU denotes relative humidity (RH) sensors. The data can be approximately taken as the degree of water saturation. The upper curve set shows the RH readings and the lower set gives the temperature.*

### 4.3.3 Total pressure at mid-height canister in the wettest hole (No 1)

The total pressure was measured by two types of gauges of which the Geokon sensors appeared to be the most accurate. The homogeneous distribution of water according to the RH measurements would correspond to a uniform distribution also of the pressure but the obvious variations in Figure 4-27 indicate that full maturation of the buffer had not taken place within 2-2.5 years. It may be that the degree of water saturation varies more than indicated by the RH measurements and also that complete, homogeneous embedment of the pressure cells requires rather long time for the involved creep, expansion, consolidation and moisture redistribution. As indicated by measurements in the Canister Retrieval Test it may well be that the cables connecting the Vaisala gauges to the recording units served as water conductors and caused local wetting and earlier saturation at the spots where the gauges are. This may explain the slight drop of RH after reaching a maximum value for one of the gauges, cf. Figure 4-26.

It is estimated that nearly complete homogeneity will require several years a main cause being that complete hydration is slower than expected.

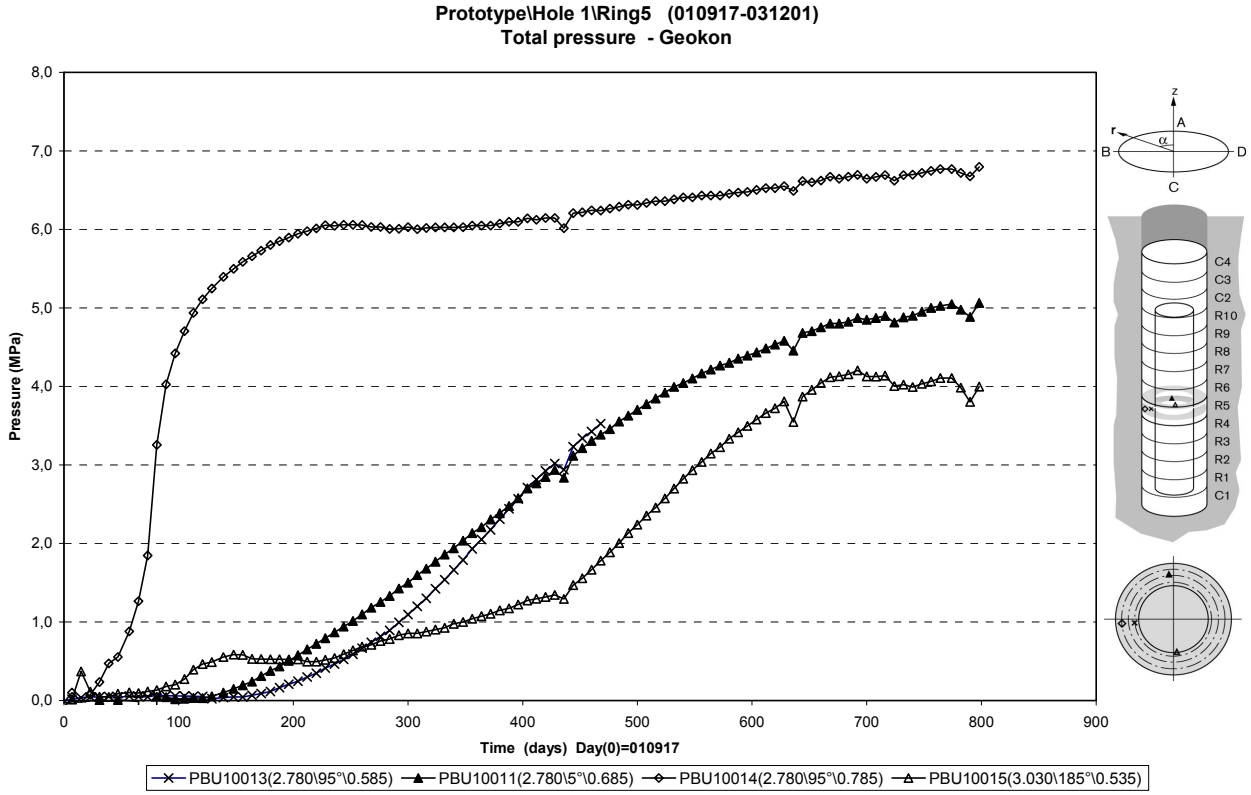


***Figure 4-27.*** *Evolution of total pressure at mid-height of the buffer in the wettest hole. The legend is explained under Figure 4-25. PBU denotes total pressure sensors. The highest pressure, about 6.7 MPa, was reached after about 2 years while the lowest (4 MPa) was obtained from a cell close to the canister in the same period of time.*

## 4.4 Comparison between predictions and recordings

### 4.4.1 General

This chapter summarizes the outcome of the various modelling attempts with respect to the evolution of temperature, hydration and total pressure, i.e. the ones that are of major importance for the practical performance of the KBS-3 concept. The results can not be compared without considering the basis of the respective calculations, which is somewhat different among the modellers. However, it is possible to get an approximate picture how the possibilities are to obtain a fairly true picture of the evolution of the buffer under different conditions with respect to the impact of the tunnel backfill and of the hydraulic performance of the rock.

### 4.4.2 Temperature evolution

The predicted and actual temperatures at the rock and the canister surface at mid-height canister level are shown in Table 4-3. One finds that two of the models give adequate data while one (THAMES) somewhat exaggerates the temperature. For BGR the canister temperature was selected and hence controlled the heat evolution of the entire buffer. For ABAQUS the boundary conditions were here set to yield maximum 83 $^{o}$C in the canister and the results were not coupled to the wetting.

**Table 4-3. Actual and expected temperature in centigrades at the canister and rock surfaces at mid-height in the wettest hole after 1 and 2 years from start.**

| Location | Recorded | COMPASS (UWC) | CODE_BRIGHT (CIMNE, Enresa) | RF/RM (BGR) | THAMES (JNC) | ABAQUS (ClayTech, SKB) |
|---|---|---|---|---|---|---|
| Canister | 1 y=69<br>2 y=72 | 1 y=70<br>2 y=72 | 1 y=70<br>2 y=72 | 1 y=100[1)]<br>2 y=100[1)] | 1 y=87<br>2 y=92 | 1 y=67[3)]<br>2 y=70[3)] |
| Rock | 1 y=56<br>2 y=60 | 1 y =56<br>2 y=59 | 1 y=57<br>2 y=60 | 1 y=92[2)]<br>2 y=96[2)] | 1 y=71<br>2 y=76 | 1 y=44<br>2 y=47 |

[1)] Set by modeller, [2)] Controlled by [1)], [3)] No real prediction. Boundary conditions set to yield maximum 83 $^{o}$C in canister and not coupled to the wetting.

### 4.4.3 Hydration

The predicted and actual degrees of saturation are difficult to compare since the uncertainty in the "measured", which could be that the actual rock conditions deviate from the assumption of unlimited access to water, see Table 4-4. Still, all the models appear to exaggerate the rate of wetting.

**Table 4-4. Actual and expected degree of saturation in percent at the canister and rock surfaces at mid-height in the wettest hole after 1 and 2 years from start.**

| Location | Recorded | COMPASS (UWC) | CODE_BRIGHT (CIMNE, Enresa) | RF/RM (BGR) | THAMES (JNC) | ABAQUS (ClayTech, SKB) |
|---|---|---|---|---|---|---|
| Canister | 1 y=90-100<br>2 y=90-100 | 1 y=96<br>2 y=100 | 1 y=95<br>2 y=97 | 1 y=76<br>2 y=84 | 1 y=79<br>2 y=99 | 1 y=75<br>2 y=100 |
| Rock | 1 y=90-100<br>2 y=90-100 | 1 y=98<br>2 y=100 | 1 y=99<br>2 y=99 | 1 y=95<br>2 y=98 | 1 y=94<br>2 y=100 | 1 y=100<br>2 y=100 |

### 4.4.4 Pressure evolution

Table 4-5 shows the predicted total pressure which deviates significantly from the actual data in some cases. The most obvious differences are found for ABAQUS, which predicts too rapid pressure build-up, and for COMPASS which predicts too slow pressure growth.

**Table 4-5. Actual and expected pressure in MPa at the canister and rock surfaces at mid-height in he wettest hole after 1 and 2 years from start.**

| Location | Recorded | COMPASS (UWC) | CODE_BRIGHT (CIMNE, Enresa) | RF/RM (BGR) | THAMES (JNC) | ABAQUS (ClayTech, SKB) |
|---|---|---|---|---|---|---|
| Canister | 1 y=1.0<br>2 y=4.0 | 1 y=0.8<br>2 y=3.2 | 1 y=3.0<br>2 y=5.1 | 1 y=3.5<br>2 y=4.8 | 1 y=4.7<br>2 y=6.2 | 1 y=5.3<br>2 y=6.8 |
| Rock | 1 y=6.0<br>2 y=6.7 | 1 y=2.8<br>2 y=3.9 | 1 y=5.0<br>2 y=7.2 | 1 y=3.5<br>2 y=4.8 | 1 y=6.4<br>2 y=7.2 | 1 y=5.3<br>2 y=6.8 |

# 5 Discussion and conclusions

## 5.1 General

In this subchapter comments by the modellers are given on the use and applicability of the respective models. The purpose is not to make assessments but to make an attempt to explain differences and deviations between predictions and actual recordings.

### 5.1.1 COMPASS (H.R Thomas and P.J Cleall, Cardiff University)

The modellers draw the following conclusions from the comparison of predicted and measured data:

- The development of the temperature regime is captured well in both Hole 1 and Hole 3. The results illustrate that the temperature regime is well understood and represented in the system. It should be noted that inclusion of the three-dimensional configuration of the 6 boreholes is essential to correctly capture the variation in the thermal response in each of the various boreholes.
- The simulated hydration rates in the buffer for Hole 1 show reasonable agreement with the experimentally measured results although some over-prediction of drying in the initial stages, (first 100 days), of the test is found. For Hole 3 it was found that the simulated hydration rates throughout the buffer showed good agreement with the experimental results measured by the Vaisala relative humidity sensors. Overall the correlation between the experimental and numerical results is encouraging.
- The simulation of the mechanical behaviour of the buffer in Hole 1 captured the key features of the observed development of swelling pressures. Peak pressures close to the rock are under-predicted possibly due to an over-estimation of the compressibility of the pellet region. In Hole 3 there is very little swelling pressure developed in both the simulated and measured results due to the slow rate of hydration experienced in this hole.

### 5.1.2 CODE_BRIGHT (A. Ledesma, CIMNE, Enresa)

The modeller draw the following conclusions from the comparison of predicted and measured data:

- The predictions of the model are reasonable when compared with the measurements. Qualitative tendencies are well reproduced, and even some numerical values are well predicted. This success is partly due to the fact that the model has been updated during the last 3 years, calibrating the parameters using the records available from the experiment. This activity has substantially improved the final model that has been used for computing THMC evolution in all the deposition holes applying a single set of parameters.

- It is clear, though, that a totally blind prediction of the experiment is still difficult to perform, due to the uncertainties related to some parameters, especially the mechanical parameters of MX-80 bentonite, which may explain the differences between measured and computed total pressures. However, despite these difficulties, the physical THM performance is quite well predicted and substantial progress has definitely been made in the numerical simulations in the last years thanks to the development of the Prototype experiment.

### 5.1.3 THAMES (Y. Sugita, JNC*)*

The modellers draw the following conclusions from the comparison of predicted and measured data:

- The prediction by THAMES is acceptable as the first step of numerical approach because it can include the principal phenomena and theories of the coupled THM behaviours expected during the re-saturation process. Compared with the actual data, some difference between the actual data and predicted results. They are solvable throughout some processes of calibration.

- The predicted temperatures were slightly higher than the monitored ones. The reason may be that the reported power of 1800 W was higher than the actual value due to power loss. Also, it may be that the thermal conductivity of the buffer is higher than assumed and that the heat transfer is assisted by some undefined mechanism like convection through vapour flow.

- The relative humidity is more difficult to predict than the temperature. Variations related to condensation and evaporation of pore water can be seen near the heater by close examination of recordings while such phenomena can not be simulated because of the difficulty to combine water diffusivity and thermal diffusivity. Nevertheless, the expected re-saturation time agrees well with measurements.

- Regarding the stress evolution, large differences between the actual data and the predicted values can be seen. One of the main reasons is that the gaps between the bentonite blocks are neglected: the initial stress in the simulation is too large compared with the actual data. Another reason is the non-linear (visco-plastic) behaviour of the buffer. In order to improve the prediction of the mechanical behaviour, further development of the code is necessary.

### 5.1.4 RF/RM (L. Liedtke, BGR)

The saturation of the bentonite buffer in the deposition hole and the overlying tunnel of the Prototype Repository Project was calculated based on the Two Phase Flow theory taking into account the excavation disturbed zones. In the calculations, a saturation test was numerically reconstructed, in situ fracture mapping in the drift were checked and surface packer tests performed. The measured water-related data in the deposition hole and the material behaviour of the bentonite are used as the basis for a numerical model. The model comprises networked 3D and 2D finite elements. The tests also included the buffer in the deposition hole, backfill in the tunnel, EDZs in the two deposition holes considered and 2 intersecting fractures. The model is coupled to the global hydraulic regime by the selection of hydraulic parameters. The mechanical stresses were calculated in parallel. The results of the hydraulic calculations, and the water saturation of the bentonite, were used when modelling the mechanical stresses. In the case of confined deformation in the margins of the deposition hole, the results indicate a build-up of stress from $P_1 = -10$ MPa. In the case of non-confined deformation after total saturation of the bentonite the largest principal stress fell to $P_1 = 0$ MPa and the two lower principal stresses to $P_{2;3} = -5$ MPa. The influence of the variation of capillary saturation is apparent in the time range (5-30 years) until saturation.

For the theoretical case with hydraulic pressure of $p_w = 1$ MPa, saturation is basically complete in the entire EDZ in the deposition hole after 10 years. In a more realistic case with water inflowing via a fracture and the EDZ, saturation is still below $S_w = 80$ % at the point in question after 30 years (Figure 5-1).

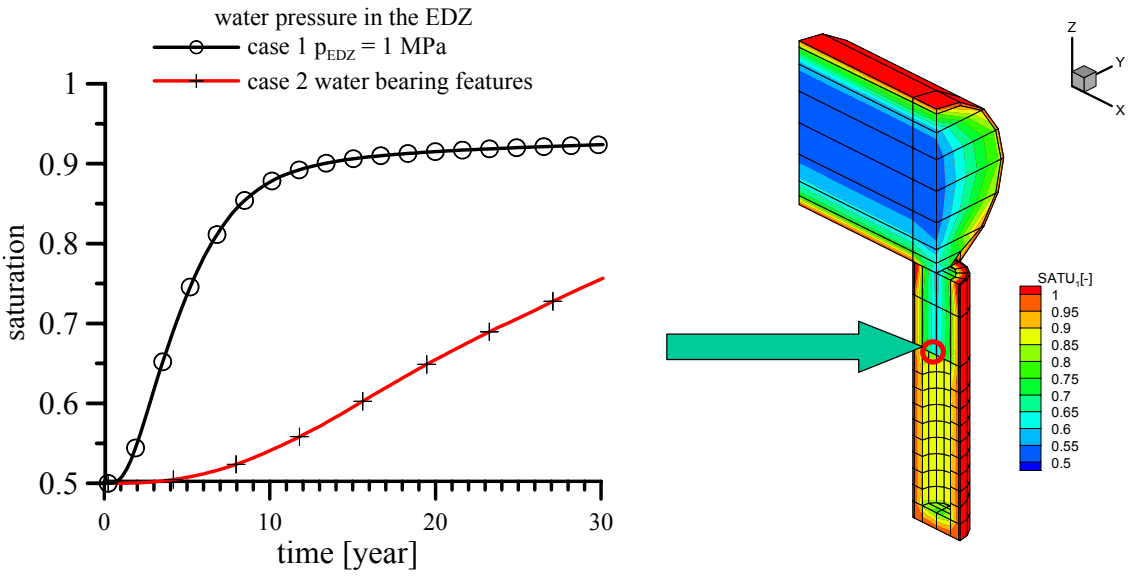


***Figure 5-1.*** *Water saturation versus time for two relevant cases.*

### 5.1.5 ABAQUS (L. Boergesson, Clay Technology, SKB)

The following conclusion can be drawn from the comparison of predicted and measured data:

- The predicted rates of the hydration and total pressure in the buffer are higher than what the recordings indicate, which may at least partly be explained because of water leakage along cables to the moisture sensors and pressure gauges.

## 5.2 Overall conclusions of the work performed

The purpose of the work has been to compare predictions made by applying the theoretical models with actual measurements and the following major conclusions can be drawn:

- The geohydraulic and geochemical modellings refer to stages that have not yet been reached in the repository test area and no safe conclusions concerning their applicability can yet be made. Predictions of access to water from the rock in the deposition holes are uncertain and future work related to rock structure on different scales appears to be required for adequate modelling of the hydration of buffers and backfills.

- All the theoretical models give data that are on the same order of magnitude as the measurements and can be used for rough prediction of the temperature, hydration and pressure build-up in buffer of the type used in the Prototype Repository Project.

- Best agreement between predictions and measurements is obtained for the temperature evolution. Some models overestimate the temperature for the first two years, hence yielding a safe, conservative prediction, while the others give very accurate forecasting. There are indications that the thermal conductivity of the buffer is higher than assumed and that the heat transfer is assisted by some undefined mechanism like convection through vapour flow.

- The hydration rate is more difficult to predict than temperature. A first and major problem is the risk of water migration along cables to moisture sensors, which may have given incorrect information on the rate of hydration of un-instrumented buffer. Thus, the reference values to be compared with the predictions may not be adequate. Disregarding from this it is concluded that almost all the models have yielded data that are fairly well in agreement with the recordings and that the models provide sufficiently safe information on the wetting rate for practical use concerning deposition holes with “unlimited” access to water from the rock. However, the predicted rate of saturation is generally too high, indicating that all processes involved in the moistening are not fully understood.

- For deposition holes with limited access to water for hydration the situation is more uncertain. One of the models could fairly accurately predict the hydration in a "dry" hole by basing the calculation on measured inflow before applying the buffer in the hole (No 3), but it seems more difficult to foresee the wetting in planning a repository with much less information on the hydraulic performance of the near-field rock. This matter should be in focus in future R&D.

- The evolution of pressure and mechanical response of the buffer is the most difficult task because it requires that fracturing and displacements in the buffer be included in the models and that the interrelation of hydration/dehydration and swelling/drying are relevant. Since prediction of the hydration rate appears to be uncertain, forecasting of the mechanical response is even more uncertain. However, the models manage to give data that are not too different from the recordings and that are sufficiently accurate for general practical purposes. Like for the hydration some pressure gauges may have reacted too soon because of water migration along cables and this may imply that the maturation of the buffer is in fact even slower than indicated by the recordings. The evolution of pressure in the buffer in "dry" deposition holes is particularly difficult to predict and stable conditions may require several tens of years according to models like the one proposed by BGR.

# 6. References

## Chapter 3

**3-1. Dershowitz, W., Winberg, A., Hermansson, J., Byegård, J., Tullborg, E-L., Andersson, P. and Mazurek, M., 2003.** Äspö Task Force on modelling of groundwater flow and transport of solutes. Task 6C. A semi-synthetic model of block-scale conductive structures at the Äspö HRL. SKB IPR-03-13. Svensk Kärnbränslehantering AB, Stockholm, Sweden.

**3-2. Rhén, I. and Forsmark, T., 2001.** Äspö Hard Rock Laboratory. Prototype Repository. Hydrogeology. Summary report of investigations before the operational phase. SKB IPR-01-65 Svensk Kärnbränslehantering AB (SKB), Stockholm, Sweden.

**3-3. Andersson, C. and Pusch, R., 2001.** Preparation of deposition holes prior to emplacement of buffer and canister in Section I. SKB IPR-01-64. Svensk Kärnbränslehantering AB, Stockholm, Sweden.

**3-4. Parkhurst, D.L. and Appelo, C.A.J., 1999.** User's guide to PHREEQC (Version 2) – A computer program for speciation, batch-reaction, one-dimensional transport, and inverse geochemical calculations. U.S. Geological Survey, Denver, Colorado. Water-Resources Investigations Report 99-4259.

**3-5. Bradbury, M.H. and Baeyens, B., 2003.** Porewater chemistry in compacted re-saturated MX-80 bentonite. Journal of Contaminant Hydrology 61: 329–338.

**3-6. Carnahan, C.L., 1987.** Simulation of chemically reactive solute transport under conditions of changing temperature. In: (ed. Tsang, C.-H.) Coupled processes associated with nuclear waste repositories. Academic Press Inc., Orlando, U.S.A., 249–257.

**3-7. Karland, O., Sandén, T., Johannesson, L.-E., Eriksen, T.E., Jansson, M., Wold, S., Pedersen, K., Motamedi, M. and Rosberg, B., 2000.** Long term test of buffer material. Final report on the pilot parcels. SKB TR-00-22. Svensk Kärnbränslehantering AB (SKB), Stockholm, Sweden.

**3-8. Muurinen, A. and Lehikoinen, J., 1999.** Porewater chemistry in compacted bentonite. Posiva Oy, Olkiluoto, Finland. Report Posiva 99-20.

**3-9. Pedersen, K., 2000.** Microbial processes in radioactive waste disposal. SKB TR TR-00-04. Svensk Kärnbränslehantering AB (SKB), Stockholm, Sweden.

## Chapter 4

**4-1. Thomas, H.R., Cleall, P.J. and Melhuish, T.A., 2002.** "Simulation of the Prototype Repository using predictive THMCB modelling" UWC contribution to D34.

**4-2. Thomas, H.R., Cleall, P.J., Chandler, N., Dixon, D. and Mitchell, H.P., 2003.** "Water infiltration into a large-scale in-situ experiment in an underground research laboratory", Geotechnique 53, No. 2, 207-224.

**4-3. Pusch, R., 1998.** "Microstructural evolution of buffer clay" In Proceedings of workshop on microstructural modelling of natural and artificially prepared clay soils with special emphasis on the use of clays for waste isolation, Lund, pp. 31-38.

**4-4. Ledesma, A. and Chen, G., 2003.** T-H-M modelling of the Prototype Repository experiment at Äspö HRL, Sweden. Proc. Geoproc Conference, KTH, Stockholm (Sweden), p. 370-375.

**4-5. Ledesma, A. and Chen, G., 2003.** THM modelling of the Prototype Repository Experiment. Comparison with current measurements. Symposium Large Scale Field Tests in Granite. Sitges (Spain), UPC, Barcelona.

**4-6. Liedtke, L., 2002.** The saturation and resulting swelling pressure of a deposition hole - tunnel system filled with bentonite under consideration of the excavation disturbed zone with the helo of two phase flow theory - ANDRA; Clays in natural and engineered barriers for radioactive waste confinement; Rheims.

**4-7. Liedtke L., Shao H., Alheid H. J. and Sönnke J., 1999.** Material Transport in Fractured Rock – Rock Characterisation in the Proximal Tunnel Zone.- Federal Institute for Geosciences and Natural Resources, Hannover.

**4-8. Thorenz, C., 2001;** Model Adaptive Simulation of Multiphase and Density Driven Flow in Fractured and Porous Media, UNI Hannover Bericht Nr. 62/2001;
ISSN 0177-9028.

**4-9. Pusch, R., 2001.** Preparation of deposition holes prior to emplacement of buffer and canister in section I; IPR-01-64, SKB, Stockholm Sweden

# Appendix 1

## Recorded power of Canister 1.